

Intercontinental dispersal and niche fidelity drive 50 million years of global diversification in *Vertigo* land snails

Michal Horsák¹  | David Ortiz¹  | Jeffrey C. Nekola¹  | Bert Van Bocxlaer² 

¹Department of Botany and Zoology,
Faculty of Science, Masaryk University,
Brno, Czech Republic

²CNRS, Univ. Lille, UMR 8198 – Evo-Eco-
Paleo, Lille, France

Correspondence

Michal Horsák, Department of Botany
and Zoology, Faculty of Science, Masaryk
University, Kotlářská 2, Brno CZ-61137,
Czech Republic.

Email: horsak@sci.muni.cz

Funding information

Czech Science Foundation, Grant/Award
Number: 20-18827S; French Agence
Nationale de la Recherche, Grant/Award
Number: ANR-17-CE02-0015

Handling Editor: Manuel Steinbauer

Abstract

Aim: We aimed to understand how biogeographical processes and moisture niche ecology contributed to the spatio-temporal diversification dynamics in the land snail genus *Vertigo*.

Location: Global (North America, Europe, Asia, Africa).

Time Period: Cenozoic era.

Major Taxa Studied: Minute terrestrial snails of the genus *Vertigo*.

Methods: We reconstructed a time-calibrated phylogeny of 94 *Vertigo* taxa (~85% of all known extant species) based on mitochondrial and nuclear DNA data. Leveraging this phylogeny with distributional and ecological data from >7000 populations, we performed biogeographic and ecological modelling to investigate evolutionary mechanisms of global *Vertigo* diversification.

Results: *Vertigo* has diversified since the Early Eocene, ca. 47.6 Ma (95% HPD = 46.0–52.7), with its six subgenera originating from the Late Eocene (30.2–48.7 Ma) to the Early Miocene (13.3–23.0 Ma). Species diversity accumulated linearly, with a slight increase 35–30 and 25–20 Ma, coinciding with the emergence of most subgenera and northern hemisphere cooling, respectively. Biogeographic modelling indicated that most diversification events occurred in sympatry (no range modification), but that rare founder events drove global diversification. Soil moisture conditions, a major variable defining *Vertigo* niches, displayed significant phylogenetic signal, but varied less among subgenera relative to within. Shifts in biogeographical ranges and moisture niches (or the absence thereof) were significantly associated at macroevolutionary scales, with most niche shifts upon sympatric cladogenesis and hardly any upon founder-event speciation.

Main Conclusions: Our results indicate that ecological shifts in soil moisture niches occasionally drove cladogenesis in sympatry and anagenetic range extensions, but that long-distance dispersal was mainly successful in the absence of such shifts. A combination of neutral (founder events and drift) and selective mechanisms (adaptive habitat shifts) has determined the macroevolutionary success of *Vertigo*. Our results

Michal Horsák and Bert Van Bocxlaer are equal contributors.

This is an open access article under the terms of the [Creative Commons Attribution-NonCommercial](https://creativecommons.org/licenses/by-nc/4.0/) License, which permits use, distribution and reproduction in any medium, provided the original work is properly cited and is not used for commercial purposes.

© 2024 The Authors. *Global Ecology and Biogeography* published by John Wiley & Sons Ltd.

imply that species with high niche fidelity or fewer opportunities for long-distance dispersal will be more vulnerable to future anthropogenic stressors.

KEYWORDS

biogeographical range estimation, comparative phylogenetics, founder-event speciation, global diversification, moisture niche, Stylommatophora

1 | INTRODUCTION

The recent increase in global distribution data and robust phylogenetic inferences offer new insights into spatio-temporal patterns of biodiversity evolution (Benson et al., 2021; Tobias et al., 2020). Vicariance caused by continental drift, mountain formation, or sea-level fluctuations has been hypothesized to be a principal diversification driver (Carta et al., 2022; Wiley, 1988). However, recent studies also highlighted that long-distance dispersal has contributed to diversification in some taxa (Matzke, 2014; Stelbrink et al., 2020). In addition, shifts in ecological niches and associated adaptation may result in barriers to gene flow among populations, potentially leading to ecological speciation (Marvaldi et al., 2002; Nosil, 2012; Schluter, 2001). At the macroevolutionary level, adaptation to new conditions after arrival may trigger adaptive evolution and radiation (Reznick & Ghahambor, 2001; Chiba, 2002; Ronco et al., 2021; but see Anderson & Weir, 2022). How neutral and selective processes contribute to diversification and what proportion of diversity has resulted from adaptation to contrasting environments (Anderson & Weir, 2022; Van Bocxlaer, 2017), remain unclear for many taxa, especially for invertebrates and taxa capable of long-distance dispersal. Studies on diversification dynamics at large spatial and temporal scales are especially lacking in land snails, because these snails often have spatially restricted distributions (Cameron, 2016; Proios et al., 2021), making it difficult to conduct global analyses across a well-defined clade.

In this context, the diverse genus *Vertigo* provides a unique opportunity to decipher global land snail diversification dynamics. *Vertigo* species have tiny body sizes (shell height varies between 1.2 and 2.7 mm) and commonly reproduce uniparentally (Pokryszko, 1987), both of which enhance their passive dispersal abilities (Nekola et al., 2018). The genus has an excellent fossil record, for example with occurrences in >200 pre-Pleistocene European fossil sites (e.g. Harzhauser & Neubauer, 2021). Because shell features allow placement of several well-preserved fossils reliably in the phylogeny (Nekola et al., 2018), fossil calibration should allow for accurate reconstruction of the tempo of *Vertigo* diversification.

Here, we generated a fossil-calibrated molecular phylogeny including >85% of all known extant *Vertigo* species, and analysed distributional and ecological data from global *Vertigo* population to study how biogeographic processes and ecology have contributed to the spatio-temporal dynamics of *Vertigo* diversification. Given the high passive dispersal capacity and global range of *Vertigo* (Nekola et al., 2018), we hypothesized that founder-event

speciation profoundly shaped *Vertigo* diversification at the macroevolutionary scale. Field data suggest that soil moisture conditions structure *Vertigo* niches (Nekola et al., 2018), as in other land snails (Juříčková et al., 2014), but how stable these niches are over long evolutionary periods is not known, nor whether shifts in moisture niches promoted diversification or how such ecological shifts relate to *Vertigo* range expansion over time. If *Vertigo* species disperse easily, but retain the same ecological niches over long periods, then we expect range expansions to have started early in the diversification history and that closely related *Vertigo* species share similar ecological niches, thus that there is less niche variation within clades than among clades.

2 | METHODS

2.1 | Taxon sampling and DNA markers

We included all 94 species and subspecies of *Vertigo* validated by a recent integrative taxonomic revision representing ~85% of the estimated extant *Vertigo* diversity (Nekola et al., 2018). For each of these taxa, we compiled distribution and ecological data from >7000 populations worldwide, allowing for documentation of intraspecific ecological variation. Geographical ranges of the species vary from very restricted (i.e. only 16 km² for *V. cupressicola*) to almost the entire northern Holarctic (*V. ronneyensis*), with most species having subcontinental distributions. Additional information on the distribution and ecology of *Vertigo* species can be found in Nekola et al. (2018). As our aim is to study diversification processes without interference from intraspecific coalescent processes, phylogenetic analyses were conducted with a single representative specimen per species or subspecies. These specimens were selected based on completeness of the molecular data and taxonomic considerations from a larger dataset with 429 individuals that included representatives from various distant populations per species to cover intraspecific genetic diversity (see Nekola et al., 2018). Many of our nucleotide sequences were already available, but some were newly generated (Table S1 in Appendix S1; see also Appendix S2 for single loci matrices). We used *Nesopupa* sp., the sister genus of *Vertigo*, as outgroup (Nekola et al., 2023). Our molecular data consisted of two mitochondrial and two nuclear DNA markers, namely cytochrome b (CYTB), 16S ribosomal RNA (16S rRNA), and Internal Transcribed Spacers 1 and 2 (after concatenation referred to as ITS), respectively. Primer sequences are provided in Table S2 in Appendix S1; for details on

gene fragments and sequence alignment see Appendix S1, M1. Each *Vertigo* taxon was represented across all four loci (there was no missing data for ingroup taxa).

2.2 | Phylogenetic inference and assessment of mitonuclear discordance

Maximum likelihood trees were obtained in IQTREE 2.2.0 (Minh et al., 2020), using two partitions for the nuclear matrix (ITS, and ITS-gaps) and four partitions for the mitochondrial matrix (CYTB-1st+2nd codon position, CYTB-3rd codon position, 16S rRNA, and 16S rRNA-gaps). The best partitioning scheme and best-fit models of substitution for each partition were determined by IQTREE through MODELFINDER (Kalyaanamoorthy et al., 2017). Branch support was obtained through 10,000 replicates of ultrafast bootstrap (Hoang et al., 2018), and values ≥ 95 were considered highly supported.

Because gene tree/species tree discordance is common at shallow phylogenetic levels (Maddison, 1997), we first conducted separate phylogenetic analyses of the mitochondrial and nuclear loci. As we did not find evidence for mitonuclear discordance in the deeper splits of *Vertigo*, that is, those reflecting subgenus relationships and directly descending diversification events, with an approximately unbiased test (see Appendix S1, M1; Figure S1 in Appendix S1, and Appendix S2 for AU test), mitochondrial and nuclear data were combined for downstream analyses to maximize support across various scales of divergence. Cases of mitonuclear discordance along shallow branches (Figure S1 in Appendix S1) could result in topological uncertainty and low support in combined analyses. The final IQTREE analysis was conducted with the same configuration per fragment as in independent gene tree analyses (see Appendix S2 for all IQTREE results).

2.3 | Divergence time estimation

Divergence time estimation was conducted in BEAST 1.10.4 (Drummond et al., 2012), with a Yule or birth-death speciation process as tree prior, and with the upper age bound on the split between *Vertigo* and *Nesopupa* as 87 or 130 Ma (see below), resulting in four analyses in total. For each analysis, four independent chains were run, each for 50 million generations, sampling every 2500, and discarding the first 25% generations as *burn-in*. Convergence between replicate runs and the effective sample size (>300) on parameter values were assessed with TRACER 1.7 (Rambaut et al., 2018). Lognormal (uncorrelated) relaxed clocks were defined for each partition. Topological constraints (see Figure S2 and M1 in Appendix S1) were applied to all clades recovered with high support in the concatenated ML analysis to reduce the tree space that was to be explored by BEAST and to increase the precision of the divergence time estimation.

Two scenarios for the upper age bound on the split between *Vertigo* and *Nesopupa* were implemented based on phylogenetic analyses of Panpulmonata with genome-wide data (Teasdale, 2017).

No representatives of Vertiginidae (to which *Nesopupa* and *Vertigo* belong) were included by Teasdale (2017), but the family belongs to Orthurethra (Nekola et al., 2023; Saadi et al., 2021) and the most basal divergence within Orthurethra was reconstructed to ~85 Ma (implemented as 87 Ma to account for uncertainty), whereas the age of the MRCA of Orthurethra and the divergent Clausilioidea was ~130 Ma. Therefore, we used 87 and 130 Ma, respectively, to constrain the maximum age of the split between *Vertigo* and *Nesopupa*. We further constrained the timing of divergence within *Vertigo* with seven reliably dated fossil calibration points that are unambiguously placed in the phylogeny (branches with high support), covering both deep and shallow divergences (Table S3 and M2 in Appendix S1). For each calibration point, we set uniform priors with the minimum age estimate of each fossil as the lowest bound for the clade that they define in the *Vertigo* phylogeny, whereas the maximum age was conservatively set to the upper bound of the split between *Vertigo* and *Nesopupa* (87 or 130 Ma, respectively). Because the age of *Vertigo* and its branching pattern were very similar regardless of the tree prior and the upper bound for the split between *Vertigo* and *Nesopupa* (Appendix S2), we used the tree generated with the simpler Yule prior and the more probable 87 Ma maximum age bound for downstream analyses (see Appendix S2). The outgroup *Nesopupa* sp. was removed for these downstream analyses.

2.4 | Analysis of diversification dynamics

The study of how biogeographic processes and ecology have contributed to the spatio-temporal dynamics of *Vertigo* diversification requires examining whether major shifts in diversification rates occurred along the phylogeny, and if so, whether such shifts relate to changes in ecology or biogeographical ranges. First, we performed lineage-through-time plots by randomly sampling 1000 trees from the posterior distribution of BEAST trees using APE v.5.6-2 (Paradis & Schliep, 2019) in R v.3.6.1 (R Core Team, 2019). Diversification patterns were compared with the 95% confidence intervals (CI) on pure birth and birth-death models parameterized from the empirical data using PHYTOOLS v.0.6-99 (Revell, 2012). We then examined whether shifts in diversification rates occurred along the *Vertigo* phylogeny with a Bayesian analysis of macroevolutionary mixtures using BAMM v. 2.5.0 (Rabosky et al., 2013). Priors for speciation and extinction rates were defined using setBAMMpriors of BAMMTOOLS v. 2.1.6. (Rabosky et al., 2014). We conducted the analyses with 10 million MCMC generations, sampling every 10,000 generations, with a burn-in of 10%. We performed three independent runs, and verified convergence by comparison of log-likelihoods over the MCMC and by calculating effective sample sizes in CODA v.0.19-3 (Plummer et al., 2006). The sampling fraction was conservatively defined as 80%, which was obtained considering the 94 included (sub) species for a total known diversity of ~110 species, supplemented with seven species that are yet to be discovered or taxonomically reassigned to *Vertigo*, including Australian *Cylindrovertilla* species (see Figure 1). We also examined whether diversification in *Vertigo*

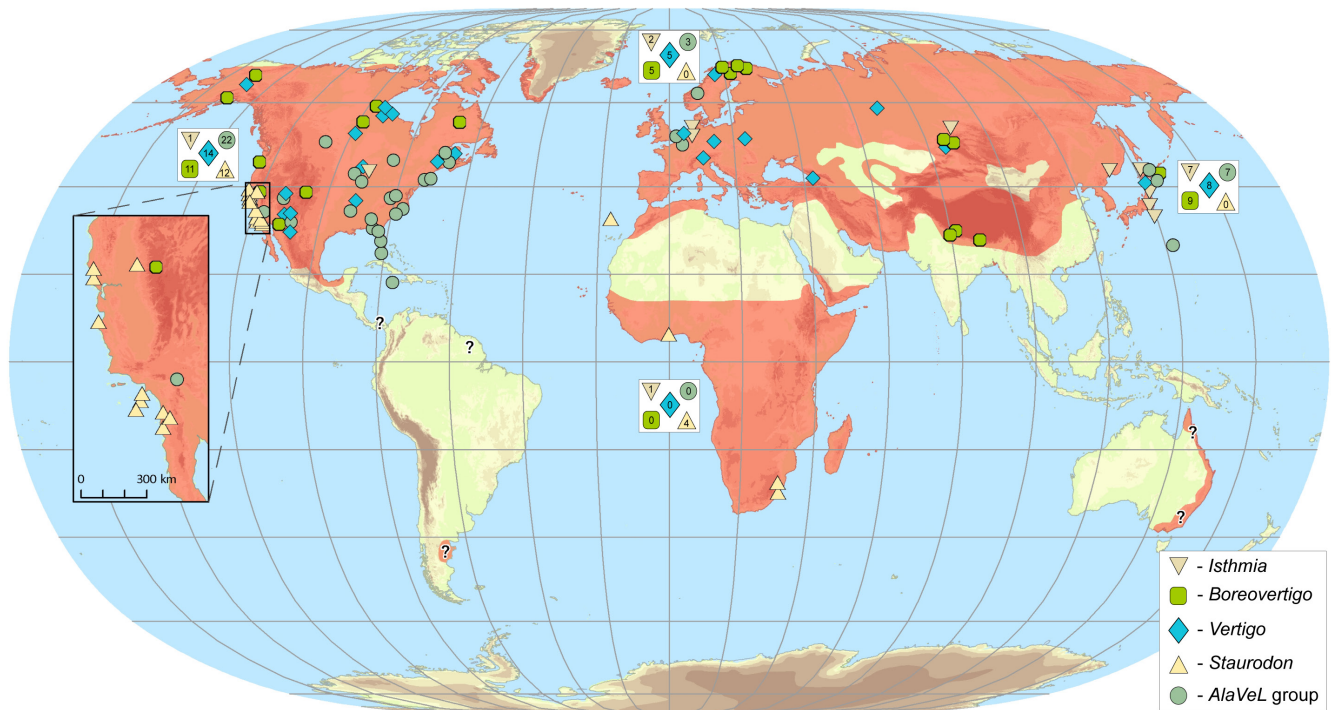


FIGURE 1 Map showing the known distribution of *Vertigo* (with minor extrapolations) as red polygons. Symbols indicate the location of all samples used in the phylogenetic analyses (see Figure 2). Panels of larger symbols in insets indicate the number of *Vertigo* species per subgenus at each continent. Question marks depict areas of distribution where *Vertigo* has never been reported, but that are occupied by taxa which likely belong to *Vertigo*.

was diversity-dependent or independent with the R package DDD v.4.1 (Etienne & Haegeman, 2019). We calculated the log-likelihood of both models and compared them with a corrected Akaike Information Criterion (AICc).

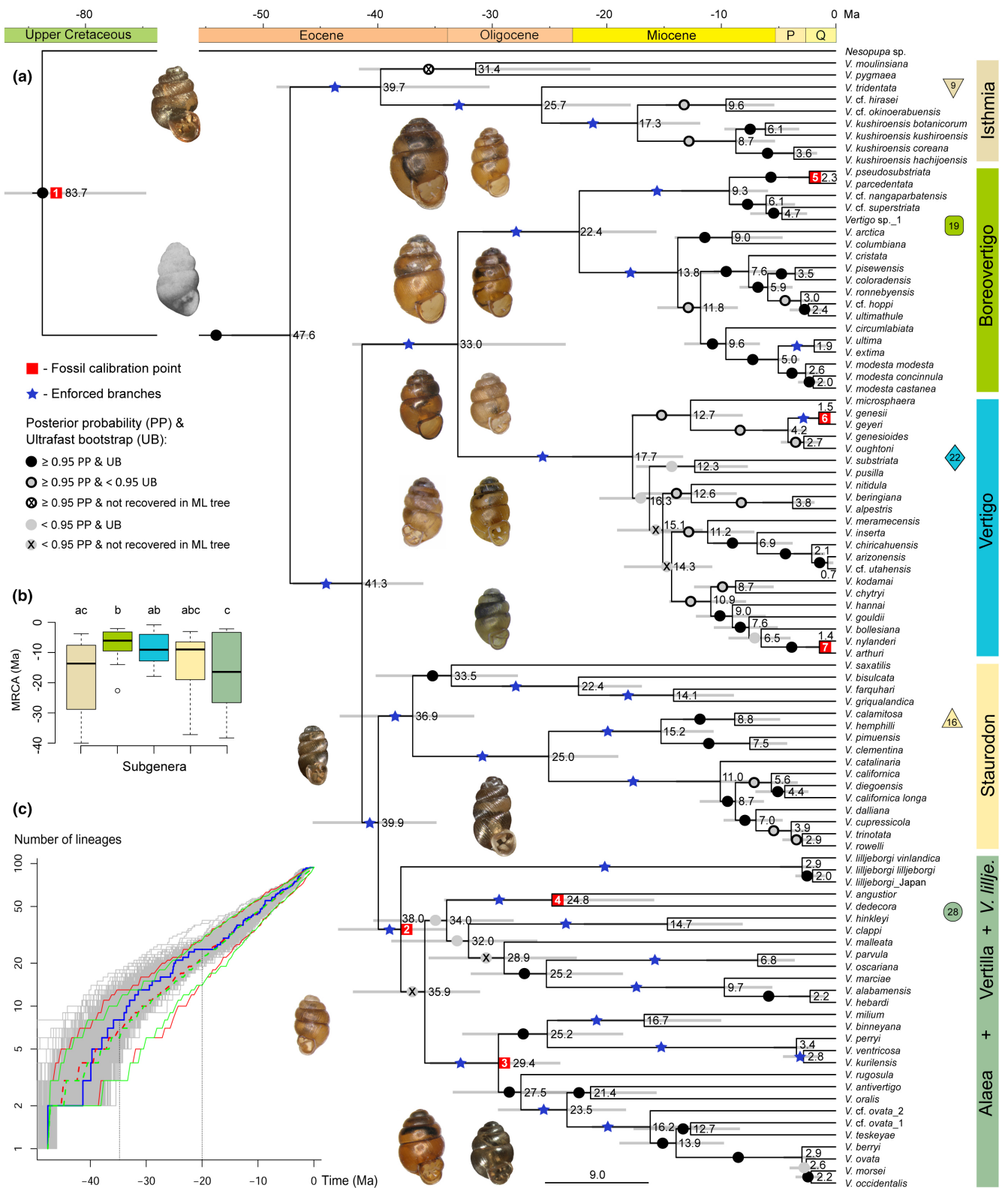
2.5 | Biogeographical analysis

We estimated ancestral ranges with a phylogenetic approach to biogeography using six reticulate models, as implemented in BioGeoBEARS v.1.1.2: DEC, DIVALIKE, and BayAreaLIKE, fitted either with or without the parameter J (Matzke, 2014, 2018, 2022), accounting for jump-dispersal at cladogenesis, therewith, integrating founder-event speciation. Model fitness among these six models was compared using AICc.

Vertigo is confirmed from four continents (North America, Europe, Asia and Africa; Figure 1) which were analysed as distributional units without further subdivision, as we intended to understand global biogeographical patterns. Species distribution data are presented in Table S1 in Appendix S1. Although Europe and Asia form a single land mass, we considered them separate due to consistent differences in climatic niche models for land snail species (see Nekola et al., 2022). Non-native occurrences, for example, the recent anthropogenic introductions of *Vertigo pygmaea* in North America, were not considered when coding geographic ranges.

Biogeographic analyses were performed with the maximum clade credibility (MCC) tree reconstructed with BEAST. As the topology of this phylogeny was not fully resolved in certain subclades, we examined the robustness of our biogeographic model comparisons and ancestral range estimations under topological uncertainty (see

FIGURE 2 (a) *Vertigo* phylogeny based on the concatenated dataset of mitochondrial (16S rRNA and COI) and nuclear (ITS1 and ITS2) markers. Branch supports from Maximum Likelihood (IQTREE) and Bayesian time-calibrated (BEAST) analyses are summarized on the BEAST tree. Values and bars on nodes represent mean node ages and 95% confidence intervals, respectively. Fossil calibration points are numbered as in Table S2 in Appendix S1. Subgenus symbols are as in Figure 1, with an indication of the number of taxa in each subgenus. Shell images represent the outgroup (*Nesopupa* sp.), the oldest known *Vertigo* shell (image adopted from Good, 1987), and the extant species (from left to right, top to bottom): *Vertigo moulinsiana*, *V. kushiorensis botanicorum*, *V. arctica*, *V. parcedentata*, *V. genesii*, *V. substriata*, *V. pusilla*, *V. chytryi*, *V. nylanderi*, *V. californica longa*, *V. calamitosa*, *V. angustior*, *V. antivertigo*, *V. ventricosa*. Shell height varies from 1.7 to 2.5 mm. (b) Variation in mean time estimates of MRCAs for all splits within subgenera; small letters indicate significant differences based on a Kruskal–Wallis test ($p=0.025$) with post-hoc pairwise Dunn's tests. (c) Cumulative number of lineages over time for 1000 trees subsampled from the BEAST posterior (grey lines), as well as for the BEAST MCC tree (blue line) compared with the mean expectations and 95% CIs under a pure birth (red) and birth-death model (green). Two vertical grey lines delimit the period with a slightly elevated number of diversification events.



Appendix S1). Specifically, we collapsed all uncertain branches and randomly resolved them after which we performed biogeographic analyses with a sample of the randomly resolved phylogenies.

We examined the role of anagenetic (dispersal, extinction) and cladogenetic biogeographic processes (sympatric divergence, subset sympatry, vicariance, and jump-dispersal) in shaping the distribution

of *Vertigo* via biogeographical stochastic mapping (BSM; Dupin et al., 2017). This analysis was performed in BioGeoBEARS with 1000 replicates and using the parameters of the best-fit biogeographic model as priors. The support for competing processes was compiled over the 1000 replicates. In certain cases, several underlying processes could explain the observed patterns. If a process received over

80% support, we considered it dominant, but alternatively, a combination of the two most supported processes was required to reach 80% support, in which case we reported the dominant process followed by the secondary process to describe biogeographic patterns.

2.6 | Analyses of moisture niche evolution

Soil humidity conditions set important constraints on *Vertigo* niches, which translate to the species occurrences (e.g. Nekola et al., 2018; Speight et al., 2003). Although moisture niches are defined along a continuous gradient, for practical reasons, we covered this gradient with three categories: xeric, mesic or wetland. Moisture niches were thus assigned based on the habitat characteristics of *Vertigo* species (Table S1 in Appendix S1). Some *Vertigo* species display intraspecific moisture niche variability and commonly occur in more than a single moisture type. Therefore, these were classified as xeric/mesic, mesic/wetland or xeric/mesic/wetland, resulting in six types of moisture niches.

We estimated ancestral moisture niches as a multistate discrete character with six states using three transition models, equal rate, symmetric rate or all rates different, and joint reconstruction as implemented in APE, and also tested for phylogenetic signal with PHYTOOLS. Secondly, because our primary goal was to examine whether changes in moisture niches are associated with alterations of biogeographic ranges or the absence thereof, we also adopted the same analytical framework as for the biogeographical analyses but with an eco-matrix coding moisture niches, rather than geographical ranges, resulting in an estimation of moisture niches as a three-state character (xeric, mesic, wetland) allowing intraspecific moisture niche variability (xeric/mesic, mesic/wetland or xeric/mesic/wetland).

Finally, we examined whether an association existed between shifts in biogeographic ranges and moisture niches, by coding along which branches range and niche shifts occurred (0=no shift; 1=shift). Subsequently, we evaluated whether shifts in biogeography and in ecology are significantly related using a χ^2 -test with contingency correction, and more specifically, whether ecological changes along branches or upon diversification are linked to specific biogeographic processes, again with χ^2 -tests.

3 | RESULTS

3.1 | Phylogenetic reconstruction

Overall, our *Vertigo* phylogeny is well-resolved and highly supported (Figure 2a). In total, 83 of 94 branches (88%) were highly supported in the BEAST phylogeny (Figure 2), 68 of which were also highly supported in the IQTREE analysis (Figure S2 in Appendix S1). Only 11 branches (12%) lacked good support in both the IQTREE and BEAST analyses. Deeper nodes and five of the six major clades of *Vertigo*, traditionally considered subgenera, were highly supported. The subgenus *Isthmia* was strongly recovered as sister to the other subgenera, which were grouped into two major clades: *Vertigo*+*Boreovertigo*, and *Staurodon*

+ (*Alaea*+*Vertilla*+*V. lilljeborgi*; i.e., the *AlaVeL* group). The basal nodes of the subgenus *Vertilla* and its relationships within the *AlaVeL* group remained unresolved. Finally, at shallower levels, some nodes, mostly within the subgenera *Isthmia* and *Vertigo*, were incompletely resolved, in part due to mitonuclear discordance (see Figure S1 in Appendix S1).

3.2 | Divergence time estimates and diversification rates

Our time-calibrated phylogeny indicates that the diversification within *Vertigo* began in the Early Eocene, ca. 47.6 Ma (95% HPD=46.0–52.7), by the split between the subgenus *Isthmia* and the rest of *Vertigo*. Time estimates for the MRCAs of *Vertigo* subgenera differed widely from the Late Eocene to Early Miocene (Figure 2a): *Isthmia* (mean time estimate=39.7 Ma; 95% HPD=30.2–48.7); *Staurodon* (36.9 Ma; 31.5–43.3); the *AlaVeL* group (38.0 Ma; 33.9–43.4); *Alaea* (29.4 Ma; 24.0–35.4); *Boreovertigo* (22.4 Ma; 15.6–30.8) and *Vertigo* (17.7 Ma; 13.3–23.0).

There was a steady accumulation of lineages through time, with a slightly elevated number of lineages in the period 35–20 Ma ago compared with average expectations under pure birth and birth-death models, but this increase remains within the 95% CI for these models (Figure 2c). The timing of within-subgenus diversification differed substantially among subgenera, as demonstrated by significant differences in the divergence times for species-level splits (Figure 2b; Kruskal-Wallis test=0.025): Species-level divergences within subgenera *Boreovertigo* and *Vertigo* were significantly younger than those within the *AlaVeL* group (Dunn test, $p < 0.038$), and those of *Boreovertigo* were also significantly younger than those of *Isthmia* ($p < 0.023$).

Our BAMM analyses all converged (ESS values were >700) towards the same result, namely that no major shifts in diversification rates occurred between clades or at any particular time in the phylogeny (Figure S3 in Appendix S1). However, speciation rates gradually decreased over time, whereas extinction rates were reconstructed as very low and constant, so that net diversification rates also gradually decreased over time. The actual number of observed *Vertigo* species is substantially below the expected number of ~220 species under the assumption of a diversity-dependent model, but model comparisons provided strong support for diversity-independent diversification (AICc weight 88.77%).

3.3 | Biogeographical range evolution

Out of the six models of range evolution (Table 1), DEC+J received the strongest support (AICc weight: 0.74), but DIVALIKE+J also received considerable support (AICc weight: 0.23). Both DEC+J and DIVALIKE+J yielded very similar parameter estimates, resulting in equivalent biological conclusions. Models consistently received much higher support when implemented with parameter +J than without it, indicating that founder-event diversification contributed strongly to range alterations in *Vertigo*. Highly similar results

TABLE 1 Results of fitting six reticulated models of *Vertigo* range evolution to our BEAST MCC phylogeny.

Model	LnL	#pars	d	e	j	AICc	AICc_wt
DEC	-141.2	2	0.008	<0.001	n.a.	286.6	<0.001
DEC+J	-132.7	3	0.005	<<0.001	0.026	271.7	0.740
DIVALIKE	-140.3	2	0.008	<<0.001	n.a.	284.7	0.001
DIVALIKE+J	-133.9	3	0.006	<<0.001	0.022	274.0	0.230
BAYAREALIKE	-177.9	2	0.006	0.027	n.a.	360.0	<<0.001
BAYAREALIKE+J	-136.2	3	0.004	<<0.001	0.039	278.7	0.023

Note: Model-fit is evaluated with a corrected Akaike information criterion and its associated weight.

Abbreviations: #pars, number of parameters; d, dispersal; e, extinction; j, jump-dispersal; LnL, Log-likelihood (base e).

were consistently retrieved upon collapsing and randomly resolving weakly supported branches in the BEAST phylogeny and refitting the biogeographical models, implying that these results are robust to uncertainty caused by mitonuclear discordance (Table S4 and Figure S4a–e in Appendix S1). Throughout all of these analyses, the extinction parameter was low, which is consistent with our BAMM results, and the similarities in the accumulation of lineages through time under pure-birth and birth-death models in *Vertigo*.

BSM indicated that most distributional range changes occurred upon cladogenesis, with only 16 out of 187 branches showing anagenetic dispersal (Figure 3). Most cladogenetic events occurred in sympatry (parameter γ ; 73 nodes of 93), followed by jump-dispersal (parameter j ; 11). Subset sympatry (parameter s) and vicariance (parameter v) were estimated as less common (6 and 3 nodes, respectively).

Although the majority of *Vertigo* diversity is known from North America (60 of 94 taxa), *Vertigo* may have originated in either North America or Eurasia (Figure 3). *Isthmia* is the only subgenus with an estimated origin in Asia, where most of its species still occur, although the subgenus is distributed across all four continents. All other subgenera have their estimated origin in North America and currently occur on two to three continents. The subgenera *Boreovertingo* and *Vertigo* show a slight dominance (ca. 60%) of species that occur in North America, whereas the subgenus *Staurodon* and the *AlaVeL* group have proportionally more North American species ($\geq 75\%$). *Staurodon* contains two main clades, however, which are reciprocally restricted to Africa and North America.

Our results indicate that long-distance dispersal occurred repeatedly across all subgenera of *Vertigo* and at all moments throughout the diversification history, from almost at the subgenus level, for example, the colonization of Africa from North America in *Staurodon*, down to sister species splits, for example, the colonization of Asia from North America by the ancestors of *Vertigo kurilensis*. Intercontinental dispersal occurred mainly from North America to other continents, except in the subgenus *Isthmia*, which colonized North America secondarily and in the subgenus *Vertigo*, where repeated range shifts involving North America, Asia, and Europe were reconstructed.

3.4 | Moisture niche evolution

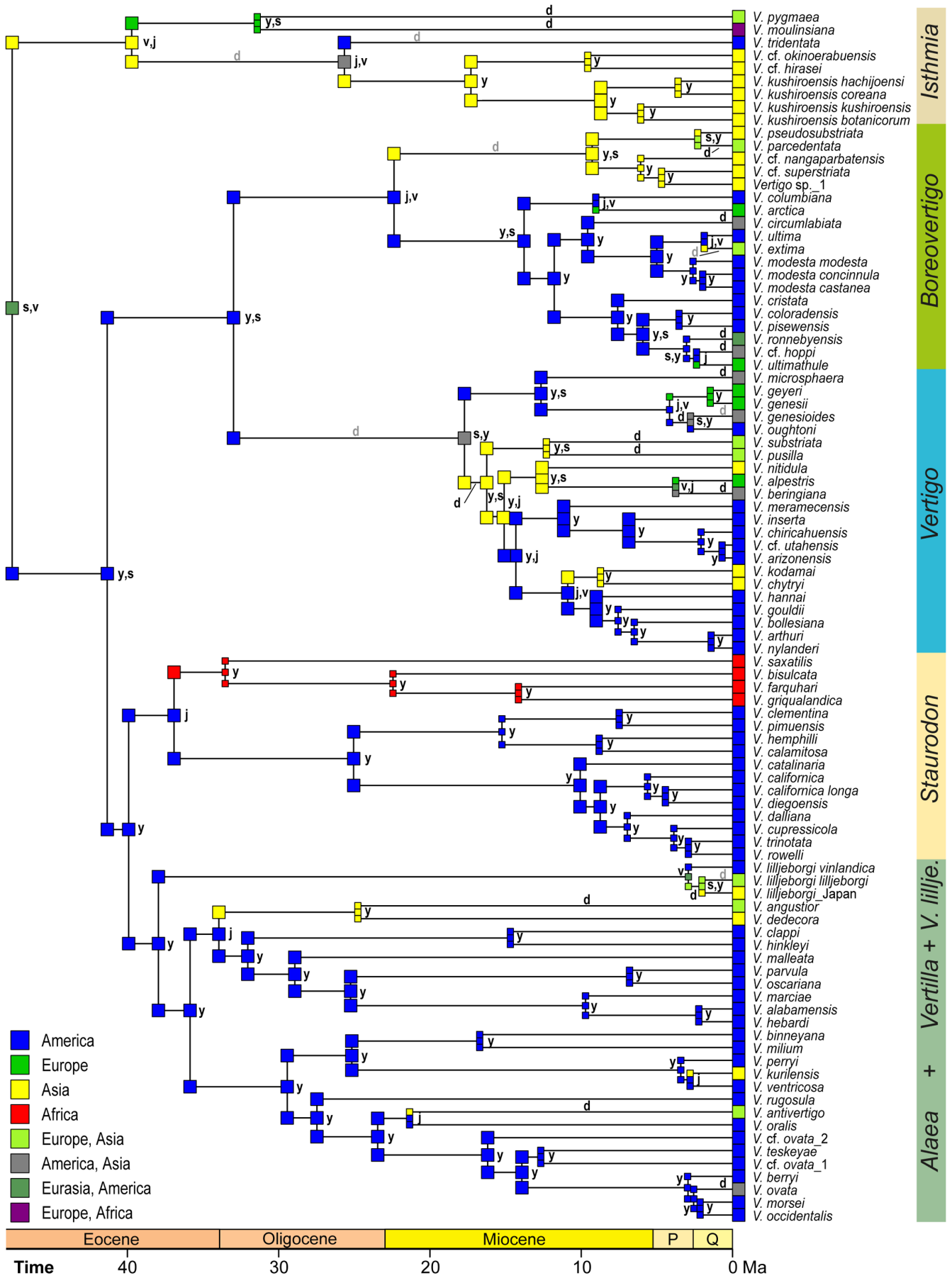
We found significant phylogenetic signal in the moisture niches of *Vertigo* species (Blomberg's $K=0.559$, $p=0.001$; Pagel's $\lambda=0.826$,

$p<0.001$). Reconstructing ancestral moisture niches as a six-state discrete character resulted in strong support for a model with a symmetric niche transition matrix (AIC weight=99.76%). This transition matrix indicated high fidelity of *Vertigo* species to moisture niches, with rare transitions occurring mainly between xeric and xeric/mesic habitats or much less frequently between mesic, mesic/wetland and wetland habitats, thus four out of 15 possible (symmetric) transition types (Figure 4b). The ancestral niche for the MRCA of *Vertigo* was most likely mesic (91.3%), although wetland (5.5%) or mesic/wetland (2.8%) conditions received some support too (Figure 4a).

Ecological modelling of moisture niches with a three-state eco-matrix and intraspecific polymorphism along the *Vertigo* phylogeny revealed results congruent with the above-mentioned approach but states that resemble those under marginal (rather than joint) ancestral state estimation (Figure S5 in Appendix S1). Under this estimation, the MRCA of *Vertigo* most likely occurred in mesic/wetland, mesic or xeric/mesic/wetland conditions. Subgenus clades of *Vertigo* are typically estimated to have occupied a mixture of mesic and wetland conditions, apart from the subgenus *Staurodon*, which would have occupied a mixture of xeric and mesic niches. With the exception of *Staurodon*, we typically found the same range of moisture niches within each subgenus; however, usually the various states were not randomly distributed among taxa within subgenus clades. Indeed, clades of related species usually share similar moisture niches (species-level splits). For example, within the *AlaVeL* group, *Alaea* was estimated to be composed almost entirely of species associated with very wet, mostly swampy habitats, which was likewise the case for the *V. lilljeborgi* subclade. However, the subgenus *Vertilla* was inferred to occupy mesic rather than wetland environments. Similarly, the majority of species in the subgenus *Vertigo* was estimated to only have inhabited mesic habitats, except for the most basally divergent subclade including the *V. genesii* group, which almost exclusively comprised species that were estimated to have occupied wetland habitats.

3.5 | Eco-evolutionary link of range and niche evolution

Upon comparing shifts in biogeographical ranges and moisture niches, we found patterns that significantly deviate from random,



- America
- Europe
- Asia
- Africa
- Europe, Asia
- America, Asia
- Eurasia, America
- Europe, Africa



Isthmia

Boreovertingo

Vertigo

Staurodon

Vertilla + V. lillje.

Alaea

FIGURE 3 *Vertigo* species-level phylogeny with ancestral range estimations obtained from fitting the DEC+J model; biogeographic processes were inferred from Bayesian stochastic mapping (BSM) with 1000 iterations. If one biogeographic process is presented at a node, it received >80% support in BSM, whereas if two processes are mentioned, the first received most support, with the joint support for both being usually >80% (and in all cases >69%). Anagenetic dispersal is represented in greyscale if it was the non-dominant process, but required to jointly reach >80% support. d, anagenetic dispersal; j, jump-dispersal; s, subset sympatry; v, vicariance; y, sympatry.

indicating an association between changes in both ($\chi^2=5.05$, $p=0.025$). Of 186 branches, 121 had no change in biogeographic range nor moisture niche, whereas in 14 cases changes in both coincided. Changes involving only biogeographic range (27 cases) or only moisture requirements (24 cases) were equally common. We also observed high stability in the moisture niche when cladogenesis was associated with jump-dispersal ($\chi^2=7.36$, $p=0.007$) and sympatry ($\chi^2=13.16$, $p<0.001$; Table 2), although changes in moisture niches upon diversification in sympatry were proportionally more common. The other biogeographic processes did not show a significant association with moisture habitats (Table 2), but at least vicariance and subset sympatry were not sufficiently common to make conclusions.

4 | DISCUSSION

Phylogenetic inference from four concatenated markers allowed us to unambiguously reconstruct the relationships between the vast majority of extant *Vertigo* species and clades. Fossil calibration of divergence times further provided robust temporal constraints to study *Vertigo* diversification in biogeographic and ecological contexts. Previous phylogenetic work on terrestrial gastropods has either been limited to smaller spatial scales (e.g. Brozzo et al., 2020; Neiber et al., 2022; Razkin et al., 2015) or featured less comprehensive sampling of included clades (e.g. de Weerd & Gittenberger, 2013; Saadi et al., 2021; Teasdale, 2017; Wade et al., 2006). In this context, our analysis of *Vertigo* diversification dynamics provides a unique opportunity to understand eco-evolutionary drivers of land snail diversification at large spatio-temporal scales.

4.1 | Time-calibrated phylogenetics reveal steady diversification with an early onset

The diversification in *Vertigo* started early compared with that of other land snail genera. The onset of diversification of snail clades considered to represent individual genera typically occurred in the last 20Ma in Clausilidae, Helicidae and Hygromiidae, but since 28.6Ma in *Oxychilus* (Neiber et al., 2022), all of which are young compared with the onset of diversification in *Vertigo* ~50Ma. *Vertigo* species accumulated steadily over time and across subgenera, with a decrease in net diversification towards the present, which is not indicative of diversity-dependent diversification, however. BAMM and biogeographic range estimations congruently indicated low extinction rates in *Vertigo*, which resulted in high similarity in pure birth and birth-death analyses. Considering methodological difficulties in

estimating extinction rates from time-calibrated phylogenies of extant taxa alone (Louca & Pennell, 2021; Morlon et al., 2011), and independent knowledge on the *Vertigo* fossil record, comprising 45 described extinct species, the inferred low extinction rates likely represent an artefact.

4.2 | Climate cooling as a driver of *Vertigo* diversification

Although *Vertigo* lineages accumulated steadily through time, we observed a slight increase in diversification 35–30Ma, related to the evolution of several subgenera, and 25–20Ma, that is, around the Oligocene–Miocene transition (~23Ma). Whereas global temperatures were reconstructed to be warm in the Late Oligocene, Early Miocene temperatures would have displayed large-scale fluctuations leading afterwards to generally cooler and dryer terrestrial ecosystems (Beddow et al., 2016; Steinhorsdottir et al., 2021). During the Miocene cooling at high and mid-latitudes, which resulted in dramatic changes in floras (Steinhorsdottir et al., 2021), the subgenera *Boreovertigo* and *Vertigo* started to diversify. This period also coincided with extensive tectonic activity and uplift of the Himalayan plateau (Spicer et al., 2021), where one of the basal clades of *Boreovertigo* primarily occurs, suggesting that it diversified there as this plateau formed. Thus, global climate change at mid- and high latitudes may have played a causal role in this increased lineage diversification in *Vertigo* around the Oligocene–Miocene transition, but the later, Pleistocene diversification dynamics of *Vertigo* also seem to be paced by glacial–interglacial climate cycles (Stewart et al., 2010). We found 13 splits with a mean reconstructed age of less than 2.6Ma, resulting in 23 taxa (16 of which are considered species). Most of these were observed in the subgenera *Boreovertigo* and *Vertigo*, consisting largely of species restricted to temperate and boreal climates. These subgenera may present an interesting study system for further population-level analyses in the context of glacial–interglacial cycles.

4.3 | Jump-dispersal shapes distributional patterns

Diversification in *Vertigo* mainly occurred in geographic sympatry, at least at continental scales, but intercontinental jump-dispersal occurred several times, mainly from North America to other continents. However, because the subgenera *Isthmia* (*V. tridentata*) has secondarily colonized North America, it seems that all biogeographic regions may act as sources for new colonization events.

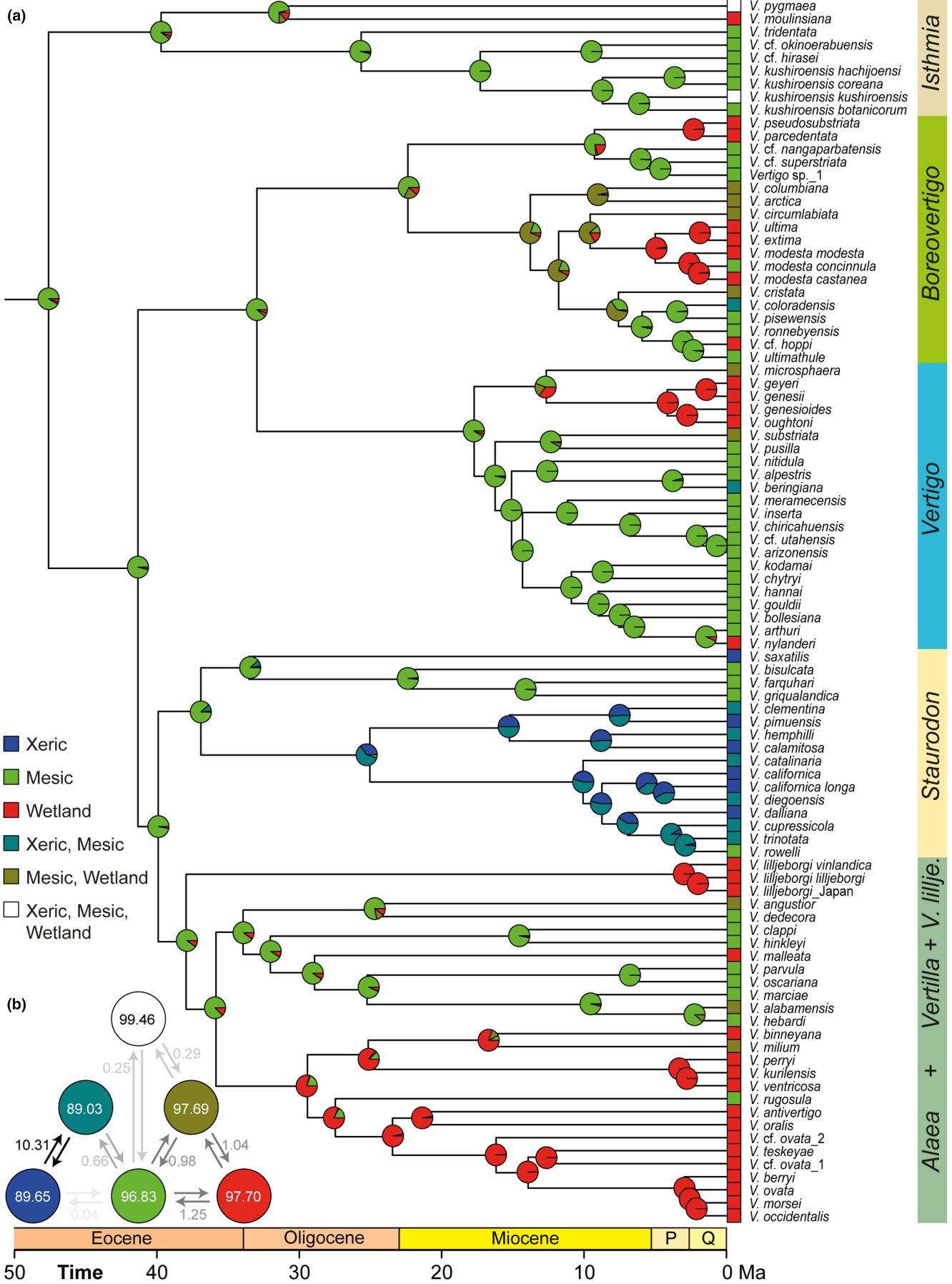


FIGURE 4 (a) Estimation of ancestral moisture-related ecological niches along the *Vertigo* phylogeny with a six-state discrete character using the best-fit symmetric transition model. (b) Graphical representation of the moisture niche transition matrix. Transition frequencies are indicated with greyscale arrows (the darker the more frequent), illustrating that only 4 out of 15 possible transition types are regularly observed.

TABLE 2 Association between ecological changes in moisture niches and range alterations.

	Vicariance	Jump-dispersal	Sympatry	Subset sympatry	Anagenetic dispersal
Stable	1	10	52	5	8
Modified	2	1	21	1	8
Significance	0.564	0.007	<0.001	0.103	1.000

Note: Moisture niches are either stable or modified upon range modifications associated with four cladogenetic processes (vicariance, jump-dispersal, sympatry, and subset sympatry) and anagenetic dispersal. Note that only dominant biogeographical processes were considered to avoid pseudoreplication. Differences were tested by χ^2 -tests under the assumption of random distribution. Significant results are in bold; the cut-off level after Bonferroni correction was $\alpha = 0.01$.

Such founder events have occurred at various times throughout the evolutionary history of *Vertigo*, impacting individual extant species, such as *V. antivertigo* and *V. kurilensis*, but older colonizations have also led to new clades, such as the African clade in the subgenus *Staurodon* or the Himalayan clade in *Boreovertigo*. This result contrasts with, for example, Viviparidae, for which founder events were also inferred, but only for deeper splits in the phylogeny (Stelbrink et al., 2020). The high capacity of long-distance dispersal and regular establishment in new regions may explain the diversity-independent nature of *Vertigo* diversification, which we had not expected as several *Vertigo* species regularly co-exist, with up to five species per site (Nekola et al., 2018).

Zoochory by migratory birds is a plausible mechanism for intercontinental dispersal, which is well-documented in the cauliid genus *Balea* that repeatedly colonized highly remote oceanic islands (Gittenberger et al., 2006). Previous studies of land and freshwater snails considered transoceanic dispersal to be very rare. They explained intercontinental distributions primarily via the disruption of larger land masses by continental drift, implying a more dominant role for vicariance (Herbert & Mitchell, 2008; Wade et al., 2006). Very few cases of vicariance were inferred for *Vertigo*, and only once as the sole inferred process, namely, the (most likely Pleistocene) segregation of three geographically isolated subspecies within the Holarctic *V. lilljeborgi* clade. Climate modelling indicates that these three subspecies occupy highly disjunct regions, separated by vast areas with unfavourable climate (Nekola et al., 2022). Although we did not find that vicariance is a main driver of diversification in *Vertigo* at the continental scale (as most continents separated prior to the origin of *Vertigo*), it still may operate at subcontinental scales, which requires further in-depth study.

4.4 | Moisture niches are conserved, with rare shifts over geological time

How ecology contributes to diversification, and whether diversification is promoted by niche conservatism versus ecological

versatility has been extensively debated, with empirical examples providing evidence for both hypotheses (Marvaldi et al., 2002; Nosil, 2012; Wiens & Graham, 2005). Niche conservatism may limit adaptation to conditions at geographic boundaries, and therewith, affect allopatric speciation (Wiens, 2004). However, in the case of frequent long-distance dispersal, niche versatility and large adaptive capabilities may be instrumental in allowing establishment and subsequent evolution in new environments. Soil moisture niches display significant phylogenetic signal in *Vertigo*, but vary more within *Vertigo* subclades than among them, indicating that habitats with different moisture conditions have been colonized rarely but repeatedly over the course of 50 Ma. Estimations of moisture niches along the phylogeny with various methods resulted in similar, robust results, with most *Vertigo* subgenera sharing mesic and wetland conditions, although one type of condition usually dominates over the other per subgenus. Xeric environments have been colonized less frequently, with *Staurodon* as a notable exception, which is the only subgenus that has successfully colonized and diversified in sub-Saharan Africa. These results indicate that *Vertigo* displays overall niche conservatism and that versatility as to moisture niches is rare, but that it has occasionally driven diversification.

4.5 | Shifts in geographic ranges and niches are associated with *Vertigo* diversification

Shifts (or the absence thereof) in biogeographic ranges and moisture niches were significantly associated at global and macroevolutionary scales. Both ranges and niches typically remain stable upon diversification, including during founder events and sympatric cladogenesis, however diversification in sympatry was more frequently associated with shifts in moisture niches (21 out of 73 cases) than in founder-event diversification (1 out of 11 cases). Changes in moisture niche were commonly associated with anagenetic dispersal (8 out of 16 cases), suggesting that ecological versatility may have promoted dispersal into new areas. From these results, we can conclude that some *Vertigo* clades and species display flexibility as to moisture niches, but

that shifts in moisture niches have rarely driven diversification and range extensions. The success of long-distance dispersal in *Vertigo* is substantially enhanced if moisture conditions are similar in the source region and the invaded range. Although our analyses focused on moisture niches, other ecological variables may have contributed to differential adaptation and speciation, and patterns of regular co-occurrence among several *Vertigo* species merit further eco-evolutionary study.

In summary, our results indicate that both neutral mechanisms, such as founder-event speciation and drift, and selective mechanisms, such as differential adaptation upon ecological niche shifts, have contributed to divergence and the evolutionary success of *Vertigo*. Whereas global ecological changes and shifts in niche preferences have occasionally promoted range shifts and diversification, such events are not the main feature of *Vertigo* diversification. The ability to disperse passively over long distances and conservatism of moisture niches upon such dispersal have strongly influenced macro-evolutionary diversification dynamics of *Vertigo*. These trajectories are determined by the patchy and often sympatric occurrence of different *Vertigo* species and the spatio-temporal dynamics by which suitable habitats emerge and disappear across the landscape (Horsák et al., 2012). In this context, increasing habitat destruction and fragmentation by humans, along with increasing climate variability due to climate change, is likely to accelerate the rate at which habitat patches become temporarily unsuitable. Such disturbance may have a particular impact on *Vertigo* species, especially those with lower dispersal capacity and those that occur in areas where habitats with favourable conditions are more patchy and/or more difficult to access.

ACKNOWLEDGEMENTS

We thank Stefan Meng for providing samples from Nepal and Ondřej Hájek for creating the distribution map. We are grateful to Thomas A. Neubauer, Frank Köhler and Björn Stelbrink for their comments on the first draft. Open access publishing facilitated by Masaryk University, as part of the Wiley - CzechELib agreement.

FUNDING INFORMATION

The study was financially supported by the Czech Science Foundation (no. 20-18827S). BVB was additionally supported by the French Agence Nationale de la Recherche through ANR-JCJC-EVOLINK (ANR-17-CE02-0015).

CONFLICT OF INTEREST STATEMENT

None.

DATA AVAILABILITY STATEMENT

All data underlying this article are provided in the Supplementary Information.

ORCID

Michal Horsák  <https://orcid.org/0000-0003-2742-2740>

David Ortiz  <https://orcid.org/0000-0001-7904-6463>

Jeffrey C. Nekola  <https://orcid.org/0000-0001-6073-0222>

Bert Van Bocxlaer  <https://orcid.org/0000-0003-2033-326X>

REFERENCES

- Anderson, S. A., & Weir, J. T. (2022). The role of divergent ecological adaptation during allopatric speciation in vertebrates. *Science*, *378*, 1214–1218.
- Beddow, H. M., Liebrand, D., Sluijs, A., Wade, B. S., & Lourens, L. J. (2016). Global change across the Oligocene-Miocene transition: High-resolution stable isotope records from IODP Site U1334 (equatorial Pacific Ocean). *Paleoceanography*, *31*, 81–97.
- Benson, R. B., Butler, R., Close, R. A., Saupe, E., & Rabosky, D. L. (2021). Biodiversity across space and time in the fossil record. *Current Biology*, *31*, R1225–R1236.
- Brozzo, A., Harl, J., De Mattia, W., Teixeira, D., Walther, F., Groh, K., Páll-Gergely, B., Glaubrecht, M., Hausdorf, B., & Neiber, M. T. (2020). Molecular phylogeny and trait evolution of Madeiran land snails: Radiation of the Geomitriini (Stylommatophora: Helicoidea: Geomitridae). *Cladistics*, *36*, 594–616.
- Cameron, R. (2016). *Slugs and snails*. HarperCollins UK.
- Carta, A., Peruzzi, L., & Ramírez-Barahona, S. (2022). A global phylogenetic regionalization of vascular plants reveals a deep split between Gondwanan and Laurasian biotas. *New Phytologist*, *233*, 1494–1504.
- Chiba, S. (2002). Ecological diversity and speciation in land snails of the genus *Mandarina* from the Bonin Islands. *Population Ecology*, *44*, 179–187.
- de Weerd, D. R. U., & Gittenberger, E. (2013). Phylogeny of the land snail family Clausiliidae (Gastropoda: Pulmonata). *Molecular Phylogenetics and Evolution*, *67*, 201–216.
- Drummond, A. J., Suchard, M. A., Xie, D., & Rambaut, A. (2012). Bayesian phylogenetics with BEAUti and the BEAST 1.7. *Molecular Biology and Evolution*, *29*, 1969–1973.
- Dupin, J., Matzke, N. J., Sarkinen, T., Knapp, S., Olmstead, R. G., Bohs, L., & Smith, S. D. (2017). Bayesian estimation of the global biogeographical history of the Solanaceae. *Journal of Biogeography*, *44*, 887–899.
- Etienne, R. S., Haegeman, B. (2019). DDD: Diversity-dependent diversification. R package, version 4.1. <https://CRAN.R-project.org/package=DDD>
- Gittenberger, E., Groenenberg, D. S. J., Kokshoorn, B., & Preece, R. C. (2006). Biogeography: Molecular trails from hitch-hiking snails. *Nature*, *439*, 409.
- Good, S. C. (1987). Mollusc-based interpretations of lacustrine paleoenvironments of the Sheep Pass Formation (latest Cretaceous to Eocene) of east central Nevada. *Palaios*, *2*, 467–478.
- Harzhauser, M., & Neubauer, T. A. (2021). A review of the land snail faunas of the European Cenozoic – Composition, diversity and turnovers. *Earth-Science Reviews*, *217*, 103610.
- Herbert, D. G., & Mitchell, A. (2008). Phylogenetic relationships of the enigmatic land snail genus *Prestonella*: The missing African element in the Gondwanan superfamily Orthalicoidea (Mollusca: Stylommatophora). *Biological Journal of the Linnean Society*, *96*, 203–221.
- Hoang, D. T., Chernomor, O., von Haeseler, A., Minh, B. Q., & Vinh, L. S. (2018). UFBoot2: Improving the ultrafast bootstrap approximation. *Molecular Biology and Evolution*, *35*, 518–522.
- Horsák, M., Hájek, M., Spitale, D., Hájková, P., Dítě, D., & Nekola, J. C. (2012). The age of island-like habitats impacts habitat specialist species richness. *Ecology*, *93*, 1106–1114.
- Juříčková, L., Horsák, M., Horáčková, J., Abraham, V., & Ložek, V. (2014). Patterns of land-snail succession in Central Europe over the last 15,000 years: Main changes along environmental, spatial and temporal gradients. *Quaternary Science Reviews*, *93*, 155–166.
- Kalyanamorthy, S., Minh, B. Q., Wong, T. K. F., von Haeseler, A., & Jermini, L. S. (2017). ModelFinder: Fast model selection for accurate phylogenetic estimates. *Nature Methods*, *14*, 587–589.
- Louca, S., & Pennell, M. W. (2021). Why extinction estimates from extant phylogenies are so often zero. *Current Biology*, *31*, 3168–3173.

- Maddison, W. P. (1997). Gene trees in species trees. *Systematic Biology*, 46, 523–536.
- Marvaldi, A. E., Sequeira, A. S., O'Brien, C. W., & Farrell, B. D. (2002). Molecular and morphological phylogenetics of weevils (Coleoptera, Curculionidae): Do niche shifts accompany diversification? *Systematic Biology*, 51, 761–785.
- Matzke, N. J. (2014). Model selection in historical biogeography reveals that founder-event speciation is a crucial process in island clades. *Systematic Biology*, 63, 951–970.
- Matzke, N. J. (2018). *BioGeoBEARS: BioGeography with Bayesian (and likelihood) evolutionary analysis with R scripts*. R package, version 1.1.2. <https://CRAN.R-project.org/package=BioGeoBEARS>
- Matzke, N. J. (2022). Statistical comparison of DEC and DEC+J is identical to comparison of two ClaSSE submodels, and is therefore valid. *Journal of Biogeography*, 49, 1805–1824.
- Minh, B. Q., Schmidt, H. A., Chernomor, O., Schrempf, D., Woodhams, M. D., von Haeseler, A., & Lanfear, R. (2020). IQ-TREE 2: New models and efficient methods for phylogenetic inference in the genomic era. *Molecular Biology and Evolution*, 37, 1530–1534.
- Morlon, H., Parsons, T. L., & Plotkin, J. B. (2011). Reconciling molecular phylogenies with the fossil record. *Proceedings of the National Academy of Sciences of the United States of America*, 108, 16327–16332.
- Neiber, M. T., Walther, F., Kijashko, P. V., Mumladze, L., & Hausdorf, B. (2022). The role of Anatolia in the origin of the Caucasus biodiversity hotspot illustrated by land snails in the genus *Oxychilus*. *Cladistics*, 38, 83–102.
- Nekola, J. C., Chiba, S., Coles, B. F., Drost, C. A., Von Proschwitz, T., & Horsák, M. (2018). A phylogenetic overview of the genus *Vertigo* O. F. Müller, 1773 (Gastropoda: Pulmonata: Pupillidae: Vertigininae). *Malacologia*, 62, 21–161.
- Nekola, J. C., Divišek, J., & Horsák, M. (2022). The nature of dispersal barriers and their impact on regional species pool richness and turnover. *Global Ecology and Biogeography*, 31, 1470–1500.
- Nekola, J. C., Nováková, M., Horsák, M., & Adema, C. M. (2023). ELAV Intron 8: A single-copy sequence marker for shallow to deep phylogeny in Eupulmonata Hasprunar & Huber, 1990 and Hygrophila Féruassac, 1822 (Gastropoda: Mollusca). *Organisms Diversity & Evolution*, 23, 621–629.
- Nosil, P. (2012). *Ecological speciation*. Oxford University Press.
- Paradis, E., & Schliep, K. (2019). ape 5.0: An environment for modern phylogenetics and evolutionary analyses in R. *Bioinformatics*, 35, 526–528.
- Plummer, M., Best, N., Cowles, K., & Vines, K. (2006). CODA: Convergence diagnosis and output analysis for MCMC. *R News*, 6, 7–11.
- Pokryszko, B. M. (1987). On aphally in the Vertiginidae (Gastropoda: Pulmonata: Orthurethra). *Journal of Conchology*, 32, 365–375.
- Proios, K., Cameron, R. A., & Triantis, K. A. (2021). Land snails on islands: Building a global inventory. *Frontiers of Biogeography*, 13, 2.
- R Core Team. (2019). *R: A language and environment for statistical computing*. R Foundation for Statistical Computing. <https://www.R-project.org/>
- Rabosky, D. L., Grudler, M. C., Anderson, C. J., Title, P. O., Shi, J. J., Brown, J. W., Huang, H., & Larson, J. G. (2014). BAMMtools: An R package for the analysis of evolutionary dynamics on phylogenetic trees. *Methods in Ecology and Evolution*, 5, 701–707.
- Rabosky, D. L., Santini, F., Eastman, J., Smith, S. A., Sidlauskas, B., Chang, J., & Alfaro, M. E. (2013). Rates of speciation and morphological evolution are correlated across the largest vertebrate radiation. *Nature Communications*, 4, e1958.
- Rambaut, A., Drummond, A. J., Xie, D., Baele, G., & Suchard, M. A. (2018). Posterior summarization in Bayesian phylogenetics using tracer 1.7. *Systematic Biology*, 67, 901–904.
- Razkin, O., Gómez-Moliner, B. J., Prieto, C. E., Martínez-Ortí, A., Arrébola, J. R., Muñoz, B., Chueca, L. J., & Madeira, M. J. (2015). Molecular phylogeny of the western Palaearctic Helicoidea (Gastropoda, Stylommatophora). *Molecular Phylogenetics and Evolution*, 83, 99–117.
- Revell, L. J. (2012). phytools: An R package for phylogenetic comparative biology (and other things). *Methods in Ecology and Evolution*, 3, 217–223.
- Reznick, D. N., & Ghalambor, C. K. (2001). The population ecology of contemporary adaptations: What empirical studies reveal about the conditions that promote adaptive evolution. *Genetica*, 112, 183–198.
- Ronco, F., Matschner, M., Böhne, A., Boila, A., Büscher, H. H., El Taher, A., Indermaur, A., Malinsky, M., Ricci, V., Kahmen, A., Jentoft, S., & Salzburger, W. (2021). Drivers and dynamics of a massive adaptive radiation in cichlid fishes. *Nature*, 589, 76–81.
- Saadi, A. J., Mordan, P. B., & Wade, C. M. (2021). Molecular phylogeny of the Orthurethra (Panpulmonata: Stylommatophora). *Zoological Journal of the Linnean Society*, 193, 1126–1140.
- Schluter, D. (2001). Ecology and the origin of species. *Trends in Ecology & Evolution*, 16, 372–380.
- Speight, M. C. D., Moorkens, E. A., & Falkner, G. (2003). Proceedings of the workshop on conservation biology of European *Vertigo* species. *Heldia*, 5, 1–183.
- Spicer, R. A., Su, T., Valdes, P. J., Farnsworth, A., Wu, F.-X., Shi, G., Spicer, T. E. V., & Zhou, Z. (2021). Why 'the uplift of the Tibetan Plateau' is a myth. *National Science Review*, 8, nwaa091.
- Steinhorsdottir, M., Coxall, H. K., De Boer, A. M., Huber, M., Barbolini, N., Bradshaw, C. D., Burls, N. J., Feakins, S. J., Gasson, E., Henderiks, J., Holbourn, A. E., Kiel, S., Kohn, M. J., Knorr, G., Kürschner, W. M., Lear, C. H., Liebrand, D., Lunt, D. J., Mörs, T., ... Strömberg, C. (2021). The Miocene: The future of the past. *Paleoceanography and Paleoclimatology*, 36, e2020PA004037.
- Stelbrink, B., Richter, R., Köhler, F., Riedel, F., Strong, E. E., Van Bocxlaer, B., Albrecht, C., Hauffe, T., Page, T. J., Aldridge, D. C., Bogan, A. E., Du, L.-N., Manuel-Santos, M. R., Marwoto, R. M., Shirokaya, A. A., & von Rintelen, T. (2020). Global diversification dynamics since the Jurassic: Low dispersal and habitat-dependent evolution explain hotspots of diversity and shell disparity in river snails (Viviparidae). *Systematic Biology*, 69, 944–961.
- Stewart, J. R., Lister, A. M., Barnes, I., & Dalén, L. (2010). Refugia revisited: Individualistic responses of species in space and time. *Proceedings of the Royal Society of London*, 277, 661–671.
- Teasdale, L. C. (2017). Phylogenomics of the pulmonate land snails. Unpublished D. Phil Thesis, University of Melbourne, Melbourne.
- Tobias, J. A., Ottenburghs, J., & Pigot, A. L. (2020). Avian diversity: Speciation, macroevolution, and ecological function. *Annual Review of Ecology, Evolution, and Systematics*, 51, 533–560.
- Van Bocxlaer, B. (2017). Hierarchical structure of ecological and non-ecological processes of differentiation shaped ongoing gastropod radiation in the Malawi Basin. *Proceedings of the Royal Society of London, Series B: Biological Sciences*, 284, 20171494.
- Wade, C. M., Mordan, P. B., & Naggs, F. (2006). Evolutionary relationships among the pulmonate land snails and slugs (Pulmonata, Stylommatophora). *Biological Journal of the Linnean Society*, 87, 593–610.
- Wiens, J. J. (2004). Speciation and ecology revisited: Phylogenetic niche conservatism and the origin of species. *Evolution*, 58, 193–197.
- Wiens, J. J., & Graham, C. H. (2005). Niche conservatism: Integrating evolution, ecology, and conservation biology. *Annual Review of Ecology, Evolution, and Systematics*, 36, 519–539.
- Wiley, E. O. (1988). Vicariance biogeography. *Annual Review of Ecology, Evolution, and Systematics*, 19, 513–542.

BIOSKETCH

Michal Horskák is a professor at Masaryk University and is interested in the ecology and phylogeny of non-marine molluscs, diversity patterns and processes of metacommunity structuring in terrestrial and aquatic systems, and the historical development of selected habitats since the LGM, reconstructed from fossil mollusc record. **Bert Van Bocxlaer** is a CNRS researcher broadly interested in patterns and processes of diversification, and associated changes in morphological disparity and ecology. He integrates data on extant and fossil biota and applies microevolutionary and macroevolutionary approaches, mainly, but not exclusively, focusing on the evolutionary radiations of freshwater molluscs in the East African Rift.

SUPPORTING INFORMATION

Additional supporting information can be found online in the Supporting Information section at the end of this article.

How to cite this article: Horskák, M., Ortiz, D., Nekola, J. C., & Van Bocxlaer, B. (2024). Intercontinental dispersal and niche fidelity drive 50million years of global diversification in *Vertigo* land snails. *Global Ecology and Biogeography*, 33, e13820. <https://doi.org/10.1111/geb.13820>

Appendix S1

Intercontinental dispersal and niche fidelity drive 50 million years of global diversification in *Vertigo* land snails

Michal Horsák, David Ortiz, Jeffrey C. Nekola, Bert Van Bocxlaer

Correspondence: horsak@sci.muni.cz

Supplementary Tables

Table S1. Species list with range and ecological information and GenBank accession numbers.

Table S2. Primer design used for PCR reactions.

Table S3. *Vertigo* fossils used for divergence time calibration.

Table S4. Results of biogeographic model-fitting accounting for topological uncertainty in *Vertigo* range evolution.

Supplementary Figures

Figure S1. Maximum likelihood phylogenies for nuclear and mitochondrial datasets.

Figure S2. Maximum likelihood phylogeny of concatenated nuclear and mitochondrial datasets with indication of branches that were enforced in downstream analyses.

Figure S3. Diversification dynamics reconstructed by Bayesian analysis of macroevolutionary mixtures.

Figure S4a-e. Examples of ancestral range estimations accounting for topological uncertainty.

Figure S5. Estimation of three-state moisture niches along the *Vertigo* phylogeny with BIOGEOBEARS.

Supplementary Methods

M1. Molecular phylogenetics.

M2. Ingroup fossil calibration points.

Supplementary Tables

Table S1. *Vertigo* species used in the phylogenetic analyses with geographical location of the specimens used for sequencing (i.e. to which the GenBank accession numbers correspond), and species-level information on range and moisture categories summarized from all examined populations (>7,000 in total).

Species name	Latitude (°N)	Longitude (°E)	Distribution	Moisture	CytB	16S	ITS1	ITS2
<i>V. alabamensis</i>	30.3680	-84.5700	America	mesic, wetland	KF214516	KF214500	KF214491	KF214479
<i>V. alpestris</i>	50.5279	13.9314	Europe	mesic	KY216926	JN941042	KY217334	KY216207
<i>V. angustior</i>	52.1826	4.4008	Europe, Asia	mesic, wetland	KY216935	KY216592	KY217343	KY216216
<i>V. antivertigo</i>	52.1590	4.4331	Europe, Asia	wetland	KY216939	KY216596	KY217347	KY216220
<i>V. arctica</i>	69.4947	20.8247	Europe	mesic, wetland	KY216944	KY216600	KY217352	KY216225
<i>V. arizonensis</i>	33.9039	-109.1619	America	mesic	KY216946	GQ921524	KY217354	GQ921580
<i>V. arthuri</i>	52.4035	-98.9119	America	mesic	KY216949	GQ921487	KY217357	KY216229
<i>V. beringiana</i>	64.6066	-149.0902	Asia, America	xeric, mesic	KY216965	GQ921515	KY217373	GQ921553
<i>V. berryi</i>	37.3743	-112.5945	America	wetland	KY216970	KY216612	KY217378	KY216243
<i>V. binneyana</i>	50.4455	-106.8520	America	wetland	KY216971	KY216613	KY217379	KY216244
<i>V. bisulcata</i>	6.3356	-0.0801	Africa	mesic	KY216973	KT008314	KY217381	KY216246
<i>V. bollesiana</i>	47.1113	-68.1316	America	mesic	KY216976	GQ921510	KY217384	GQ921575
<i>V. calamitosa</i>	32.6730	-117.2449	America	xeric	KY216987	KY216625	KY217395	KY216258
<i>V. californica</i>	38.3492	-123.0659	America	xeric	KY216993	KY216629	KY217401	KY216264
<i>V. californica longa</i>	32.9953	-118.5516	America	xeric	KY216999	KY216635	KY217407	KY216270
<i>V. catalinaria</i>	33.3456	-118.4419	America	xeric, mesic	KY217011	KY216647	KY217419	KY216282
<i>V. cf. hirasei</i>	38.6740	141.1103	Asia	mesic	KY217136	KY216750	KY217537	KY216395
<i>V. cf. hoppi</i>	58.7333	-93.8069	Asia, America	wetland	KY217139	KY216753	KY217540	KY216398
<i>V. cf. nangaparatensis</i>	29.8872	81.6444	Asia	mesic	OR051761	OR039426	OR039439	OR039445
<i>V. cf. okinoerabuensis</i>	35.6325	139.4677	Asia	mesic	KY217237	KY216837	KY217636	KY216491
<i>V. cf. ovata_1</i>	34.9345	-77.0100	America	wetland	KY217251	KY216850	KY217649	KY216504

<i>V. cf. ovata_2</i>	41.9019	-70.8521	America	wetland	KY217248	KY216848	KY217647	KY216502
<i>Vertigo</i> sp._1	27.7352	87.9697	Asia	mesic	OR051762	OR039427	OR039440	OR039446
<i>V. cf. superstriata</i>	29.8854	80.7968	Asia	mesic	OR051763	OR039428	OR039441	OR039447
<i>V. cf. utahensis</i>	38.4171	-112.3126	America	mesic	KY217326	KY216918	KY217716	KY216577
<i>V. circumlabiata</i>	43.7527	144.8426	Asia, America	mesic, wetland	KY217025	KY216660	KY217433	KY216296
<i>V. clappi</i>	38.0631	-79.8885	America	mesic	KY217032	KY216666	KY217438	KY216303
<i>V. clementina</i>	32.9953	-118.5516	America	xeric, mesic	KY217033	KT008325	KY217439	KY216304
<i>V. coloradensis</i>	32.4413	-110.7848	America	xeric, mesic	KY217041	GQ921540	KY217447	GQ921587
<i>V. columbiana</i>	45.6413	-123.9410	America	mesic, wetland	KY217045	KY216676	KY217451	KY216315
<i>V. cristata</i>	55.0647	-67.2348	America	mesic, wetland	KY217053	GQ921544	KY217459	GQ921584
<i>V. cupressicola</i>	36.5782	-121.9727	America	xeric, mesic	KY217057	KY216684	KY217461	KY216324
<i>V. dalliana</i>	38.7396	-123.2446	America	xeric	KY217061	KY216688	KY217465	KY216328
<i>V. dedecora</i>	26.6537	142.1536	Asia	mesic	KY217066	KY216691	KY217469	KY216332
<i>V. diegoensis</i>	32.6720	-117.2449	America	xeric, mesic	KY217070	KY216694	KY217473	KY216336
<i>V. extima</i>	69.6612	25.8886	Europe, Asia	wetland	KY217087	KY216712	KY217490	KY216353
<i>V. farquhari</i>	-29.8149	31.0174	Africa	mesic	KY217090	KY216715	KY217492	KY216356
<i>V. genesii</i>	46.6741	10.3522	Europe	wetland	KY217097	KY216721	KY217499	KY216362
<i>V. genesioides</i>	58.6464	-93.8245	Asia, America	wetland	KY217104	KY216728	KY217506	KY216369
<i>V. geyeri</i>	51.1568	23.6000	Europe	wetland	KY217108	KY216732	KY217510	KY216373
<i>V. gouldii</i>	42.7796	-91.6890	America	mesic	KF214508	GQ921506	KF214484	KF214472
<i>V. griqualandica</i>	-27.5274	30.7276	Africa	mesic	KY217117	KY216739	KY217519	KY216382
<i>V. hannai</i>	58.7447	-93.8716	America	mesic	KY217122	GQ921520	KY217523	GQ921573
<i>V. hebardei</i>	24.8146	-80.8211	America	mesic	KF214511	KF214505	KF214487	KF214475
<i>V. hemphilli</i>	32.5428	-117.1061	America	xeric, mesic	KY217129	KT008331	KY217530	KY216389
<i>V. hinkleyi</i>	31.4105	-110.2824	America	mesic	KY217134	GQ921545	KY217535	GQ921592
<i>V. chiricahuensis</i>	30.6003	-109.2199	America	mesic	KY217017	GQ921526	KY217425	KY216288
<i>V. chytryi</i>	58.5269	68.6815	Asia	mesic	KY217023	KY216658	KY217431	KY216294
<i>V. inserta</i>	33.9039	-109.1619	America	mesic	KY217145	GQ921529	KY217547	GQ921578
<i>V. kodamai</i>	42.1815	143.0003	Asia	mesic	KY217152	KY216764	KY217554	KY216410
<i>V. kurilensis</i>	43.0817	144.8442	Asia	wetland	KY217155	KY216767	KY217558	KY216414

<i>V. kushiroensis</i>	43.0340	144.3901	Asia	xeric, mesic, wetland	KY217162	KY216774	KY217565	KY216421
<i>V. kushiroensis botanicorum</i>	51.5074	85.5968	Asia	mesic	KY216978	KY216616	KY217386	KY216249
<i>V. kushiroensis coreana</i>	43.6971	132.1633	Asia	mesic	KY217147	KY216759	KY217549	KY216405
<i>V. kushiroensis hachijoensis</i>	33.1320	139.6805	Asia	mesic	KY217120	KY216741	KY217521	KY216384
<i>V. lilljeborgi</i>	62.3558	9.6832	Europe, Asia	wetland	KY217172	KY216784	KY217575	KY216431
<i>V. lilljeborgi (Japan)</i>	43.9200	144.1586	Asia	wetland	KY217169	KY216781	KY217572	KY216428
<i>V. lilljeborgi vinlandica</i>	46.7850	-68.5408	America	wetland	KY217176	KY216788	KY217579	KY216435
<i>V. malleata</i>	34.5492	-77.7817	America	wetland	KY217178	KT008318	KY217581	KY216437
<i>V. marciae</i>	18.1132	-76.6685	America	mesic	KF214514	KF214502	KF214489	KF214477
<i>V. meramecensis</i>	36.7931	-91.3334	America	mesic	KY217186	KY216793	KY217588	KY216443
<i>V. microsphaera</i>	50.9855	85.6817	Asia, America	mesic, wetland	KY217195	KY216802	KY217597	KY216452
<i>V. milium</i>	42.3764	-91.8507	America	mesic, wetland	KY217200	KT008328	KY217602	KY216457
<i>V. modesta castanea</i>	38.7900	-120.0093	America	wetland	KY217214	KY216820	KY217614	KY216472
<i>V. modesta concinnula</i>	38.7171	-106.4987	America	mesic	KY217049	KY216679	KY217455	KY216318
<i>V. modesta modesta</i>	67.0197	-150.2886	America	wetland	KY217212	KY216818	KY217612	KY216470
<i>V. morsei</i>	46.0754	-83.6684	America	wetland	KY217212	KY216818	KY217612	KY216470
<i>V. moulinsiana</i>	52.1710	4.6119	Africa, Europe	wetland	KY217225	KT008326	KY217625	KY216483
<i>V. nitidula</i>	41.9274	42.7498	Asia	mesic	KY217229	KY216833	KY217628	KY216486
<i>V. nylanderii</i>	46.6120	-68.5953	America	wetland	KY217233	GQ921483	KY217632	GQ921576
<i>V. occidentalis</i>	34.2230	-116.9410	America	wetland	KY217235	KY216836	KY217634	KY216489
<i>V. oralis</i>	27.4726	-81.5550	America	wetland	KY217239	KY216839	KY217638	KY216493
<i>V. oscariana</i>	32.5481	-85.4855	America	mesic	KY217242	KY216842	KY217641	KY216496
<i>V. oughtoni</i>	58.7264	-94.1171	America	wetland	KY217243	KY216843	KY217642	KY216497
<i>V. ovata</i>	42.2815	-91.8323	Asia, America	wetland	KY217246	KY216846	KY217645	KY216500
<i>V. parcedentata</i>	50.1510	88.3031	Europe, Asia	wetland	KY217254	KY216853	KY217652	KY216507
<i>V. parvula</i>	37.9272	-79.9861	America	mesic	KY217260	KY216859	KY217657	KY216512
<i>V. perryi</i>	41.9010	-70.8521	America	wetland	KY217262	KY216861	KY217659	KY216514
<i>V. pimuensis</i>	33.4458	-118.4817	America	xeric	KY217264	KY216863	KY217661	KY216516
<i>V. pisewensis</i>	55.1982	-98.3918	America	mesic	KY217267	KY216866	KY217664	KY216519
<i>V. pseudosubstriata</i>	50.9855	85.6817	Asia	wetland	KY217271	KT008317	KY217668	KY216523

<i>V. pusilla</i>	69.2193	19.9587	Europe, Asia	mesic	KF214520	KF214496	KY217671	KF214483
<i>V. pygmaea</i>	52.1590	4.4331	Europe, Asia	xeric, mesic, wetland	KY217280	KY216877	KY217678	KY216532
<i>V. ronneyensis</i>	69.1911	19.9873	Europe, Asia, America	mesic	KY217285	KY216882	KY217682	KY216537
<i>V. rowelli</i>	38.9072	-121.0516	America	mesic	KY217296	KT008327	KY217689	KY216548
<i>V. rugosula</i>	34.4040	-92.1020	America	mesic	KY217302	KT008319	KY217695	KY216554
<i>V. saxatilis</i>	32.6928	-16.8044	Africa	xeric	KY217304	KY216897	KY217697	KY216556
<i>V. substriata</i>	52.4413	4.6267	Europe, Asia	mesic, wetland	KY217308	KY216901	KY217700	KY216560
<i>V. teskeyae</i>	29.7951	-82.7659	America	wetland	KY217312	KY216904	KY217703	KY216563
<i>V. tridentata</i>	42.1795	-90.9979	America	mesic	KY217315	KY216907	KY217706	KY216566
<i>V. trinotata</i>	36.5782	-121.9727	America	xeric, mesic	KY217318	KY216910	KY217709	KY216569
<i>V. ultima</i>	61.1997	-149.9667	America	wetland	KY217320	KY216912	KY217711	KY216571
<i>V. ultimathule</i>	69.6612	25.8886	Europe	mesic	KY217324	KY216916	KY217714	KY216575
<i>V. ventricosa</i>	46.9004	-68.2466	America	wetland	KY2129	KY2121	KY2119	KY2180

Table S2. Primers used for PCR reactions, and their associated annealing temperature (adopted from Nekola et al. 2018).

Amplicon/Name	Sequence	Anneal (°C)	Source
CytB			
CytB397f	5' – YWYTRCCTTGGRGGRCARATATC – 3'	47	Dahlgren et al. (2000)
CytBfV	5' – TGAGGTGCAACAGTNATTAC – 3'	47	Nekola et al. (2018)
CytBfVU	5' – GGNCAAATRTCATTTTGAGGNGC – 3'	47	Nekola et al. (2018)
CytBfext	5' – CATATTGGTCGGGGRTTATACTA – 3'	47	Nekola et al. (2018)
CytB811r	5' – GCRWAYARAAAARTAYCAYTCWGG – 3'	47	Dahlgren et al. (2000)
CytBrV	5' – GCAAATAAAAAATATCATTTCAGG – 3'	47	Nekola et al. (2018)
CytBrVU	5' – TGATCGTAAAATRGCATATGCA – 3'	47	Nekola et al. (2018)
16S rRNA			
16Sar	5' – GCGCTGTTTATCAAAAACAT – 3'	52	Palumbi (1996)
16SfV	5' – CACCTGTTTAAACAAAAACA – 3'	52	Nekola et al. (2018)
16SfVjap	5' – CGACTGTTTAGCAAAAACA – 3'	52	Nekola et al. (2018)
16SfVG	5' – TAAGGAACTCGGCAAAMAT – 3'	52	Nekola et al. (2018)
16Sbr	5' – CCGGYTGAAGTCAAGATCAYGT – 3'	52	Tongkerd et al. 2004
16SrPUm	5' – GGCTTACGCCGGTCTGAACTC – 3'	52	Nekola et al. (2018)
ITS1			
18srDNA	5' – TAACAAGGTTTCCGTATGTGAA – 3'	52	Armbruster & Bernhard (2000)
LSU1rc	5' – TCACATTAATTCTCGCAGCTAG – 3'	52	Nekola et al. (2018)
ITS2			
LSU1	5' – CTAGCTGCGAGAATTAATGTGA – 3'	52	Wade & Mordan (2000)
LSU3	5' – ACTTCCCTCACGGTACTTGG – 3'	52	Wade & Mordan (2000)
LSU3rm	5' – GGTTTCACGTAAGTCTTGAAC – 3'	52	Nekola et al. (2018)

References

- Armbruster, G. F. J., Bernhard, D. (2000). Taxonomic Significance of Ribosomal ITS-1 Sequence Markers in Self-fertilizing Land Snails of *Cochlicopa* (Stylommatophora, Cochlicopidae). *Zoosystematics & Evolution*, 76, 11–18.
- Dahlgren, T. G., Weinberg, J. R., Halanych, K. M. (2000). Phylogeography of the ocean quahog (*Arctica islandica*): influences of paleoclimatic on genetic diversity and species range. *Marine Biology*, 137, 487–495.
- Nekola, J. C., Chiba, S., Coles, B. F., Drost, C. A., Von Proschwitz, T., Horsák, M. (2018). A phylogenetic overview of the genus *Vertigo* O. F. Müller, 1773 (Gastropoda: Pulmonata: Pupillidae: Vertigininae). *Malacologia*, 62, 21–161.
- Palumbi, S. R. (1996). *Nucleic Acids II: The Polymerase Chain Reaction*. Pp. 205–247 In: D. M. Hillis, C. Moritz, B. K. Mable, Eds., *Molecular Systematics*, Edition 2 (Sinauer Associates, Sunderland).
- Tongkerd, P., Lee, T., Panha, S., Burch, J. B., O'foighil, D. (2004). Molecular phylogeny of certain Thai Gastrocoptinae micro land snails (Stylommatophora: Pupillidae) inferred

from mitochondrial and nuclear ribosomal DNA sequences. *Journal of Molluscan Studies*, 70, 139–147.

Wade, C. M., Mordan, P. B. (2000). Evolution within the gastropod Molluscs; using the ribosomal RNA gene-cluster as an indicator of phylogenetic relationships. *Journal of Molluscan Studies*, 66, 565–570.

Table S3. *Vertigo* fossils used for divergence time calibration, with ages in Ma. Details about individual fossils and reasoning of their selection are provided below (see section M2).

	Original name	Clade calibrated	Max. age	Min. age	References
1	<i>Vertigo</i> sp.	MRCA of all <i>Vertigo</i>	50.30	46.20	Good (1987)
2	<i>V. vectensis</i>	MRCA of clades <i>Alaea</i> + <i>Vertilla</i> + <i>V. lilljeborgi</i>	37.71	33.90	Cox (1924)
3	<i>V. ovatula</i>	MRCA of subgenus <i>Alaea</i>	27.82	23.03	Stworzewicz (1999)
4	<i>V. angustior</i>	<i>V. angustior</i> + <i>V.</i> <i>dedecora</i>	15.97	12.70	Harzhauser and Neubauer (2021)
5	<i>V. parcedentata</i>	<i>V. parcedentata</i> + <i>V.</i> <i>pseudosubstriata</i>	1.20	1.20	Stworzewicz et al. (2012)
6	<i>V. genesii</i>	<i>V. genesii</i> + <i>V. geyeri</i>	1.20	1.20	Stworzewicz et al. (2012)
7	<i>V. nylanderi</i>	<i>V. nylanderi</i> + <i>V. arthuri</i>	0.83	0.73	Miller et al. (1994)

Table S4. Results of fitting six reticulated models of *Vertigo* range evolution to five phylogenies, each obtained after randomly resolving the BEAST phylogeny in which weakly supported branches had been collapsed. Abbreviations: LnL, Log-likelihood (base e); #par, number of parameters; d, dispersal; e, extinction; j, jump-dispersal. Model-fit is evaluated with a corrected Akaike information criterion, and its associated weight.

Model	LnL	#pars	d	e	j	AICc	AICc_wt
Tree 1 (Figure S4a)							
DEC	-144.3	2	0.008	0.002	n.a.	292.7	<0.001
DEC+J	-133.8	3	0.005	<<0.001	0.028	273.9	0.620
DIVALIKE	-142.9	2	0.008	0.002	n.a.	289.9	<0.001
DIVALIKE+J	-134.3	3	0.006	<<0.001	0.023	274.9	0.370
BAYAREALIKE	-179.4	2	0.006	0.027	n.a.	362.9	<<0.001
BAYAREALIKE+J	-138.4	3	0.004	<<0.001	0.039	283.0	0.007
Tree 2 (Figure S4b)							
DEC	-142.2	2	0.007	0.002	n.a.	288.6	<0.001
DEC+J	-133.4	3	0.005	<<0.001	0.026	273.0	0.760
DIVALIKE	-142.4	2	0.008	0.001	n.a.	289.0	<0.001
DIVALIKE+J	-134.5	3	0.006	<<0.001	0.024	275.3	0.237
BAYAREALIKE	-179.2	2	0.006	0.027	n.a.	362.5	<<0.001
BAYAREALIKE+J	-138.8	3	0.004	<<0.001	0.042	284.0	0.003
Tree 3 (Figure S4c)							
DEC	-143.7	2	0.008	0.002	n.a.	291.4	<<0.001
DEC+J	-132.9	3	0.005	<<0.001	0.027	272.1	0.727
DIVALIKE	-144.3	2	0.008	0.001	n.a.	292.7	<<0.001
DIVALIKE+J	-133.9	3	0.006	<<0.001	0.023	274.1	0.267
BAYAREALIKE	-179.2	2	0.006	0.027	n.a.	362.6	<<0.001
BAYAREALIKE+J	-137.7	3	0.004	<<0.001	0.038	281.6	0.006
Tree 4 (Figure S4d)							
DEC	-143.1	2	0.008	0.002	n.a.	290.2	<<0.001
DEC+J	-132.8	3	0.005	<<0.001	0.027	271.9	0.630
DIVALIKE	-143.6	2	0.008	0.002	n.a.	291.3	<<0.001
DIVALIKE+J	-133.4	3	0.006	<<0.001	0.024	273.1	0.360
BAYAREALIKE	-179.3	2	0.006	0.027	n.a.	362.7	<<0.001
BAYAREALIKE+J	-137	3	0.004	<<0.001	0.038	280.3	0.010
Tree 5 (Figure S4e)							
DEC	-141.6	2	0.007	<0.001	n.a.	287.4	<0.001
DEC+J	-133.3	3	0.005	<<0.001	0.026	272.8	0.838
DIVALIKE	-141.5	2	0.008	<<0.001	n.a.	287.2	<0.001
DIVALIKE+J	-134.9	3	0.006	<<0.001	0.024	276.1	0.158
BAYAREALIKE	-179.2	2	0.006	0.027	n.a.	362.5	<<0.001
BAYAREALIKE+J	-138.7	3	0.004	<<0.001	0.040	283.6	0.004

Supplementary Figures

nDNA (ITS1 and ITS2)

mtDNA (CytB and 16S)

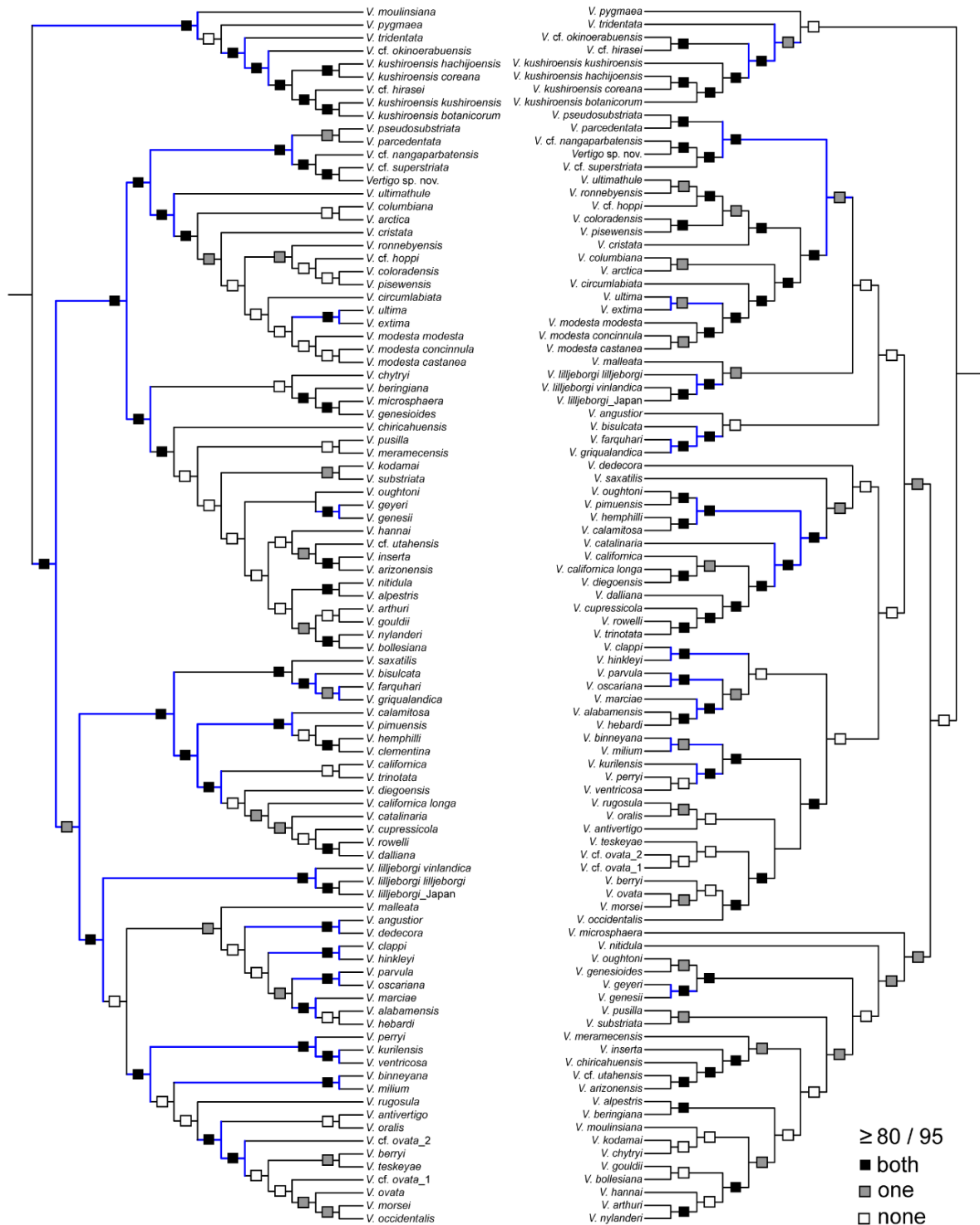


Figure S1. Maximum likelihood nuclear ITS (left) and mitochondrial (right) trees of *Vertigo*. Square color represents branch support obtained through Ultrafast bootstrap (high support: ≥ 95) and the aLRT-SH test (≥ 80). Blue branches were enforced in the downstream concatenated analyses after mitonuclear discordance was discarded by an AU test. To improve visibility, the outgroup was removed and branch length information was discarded.

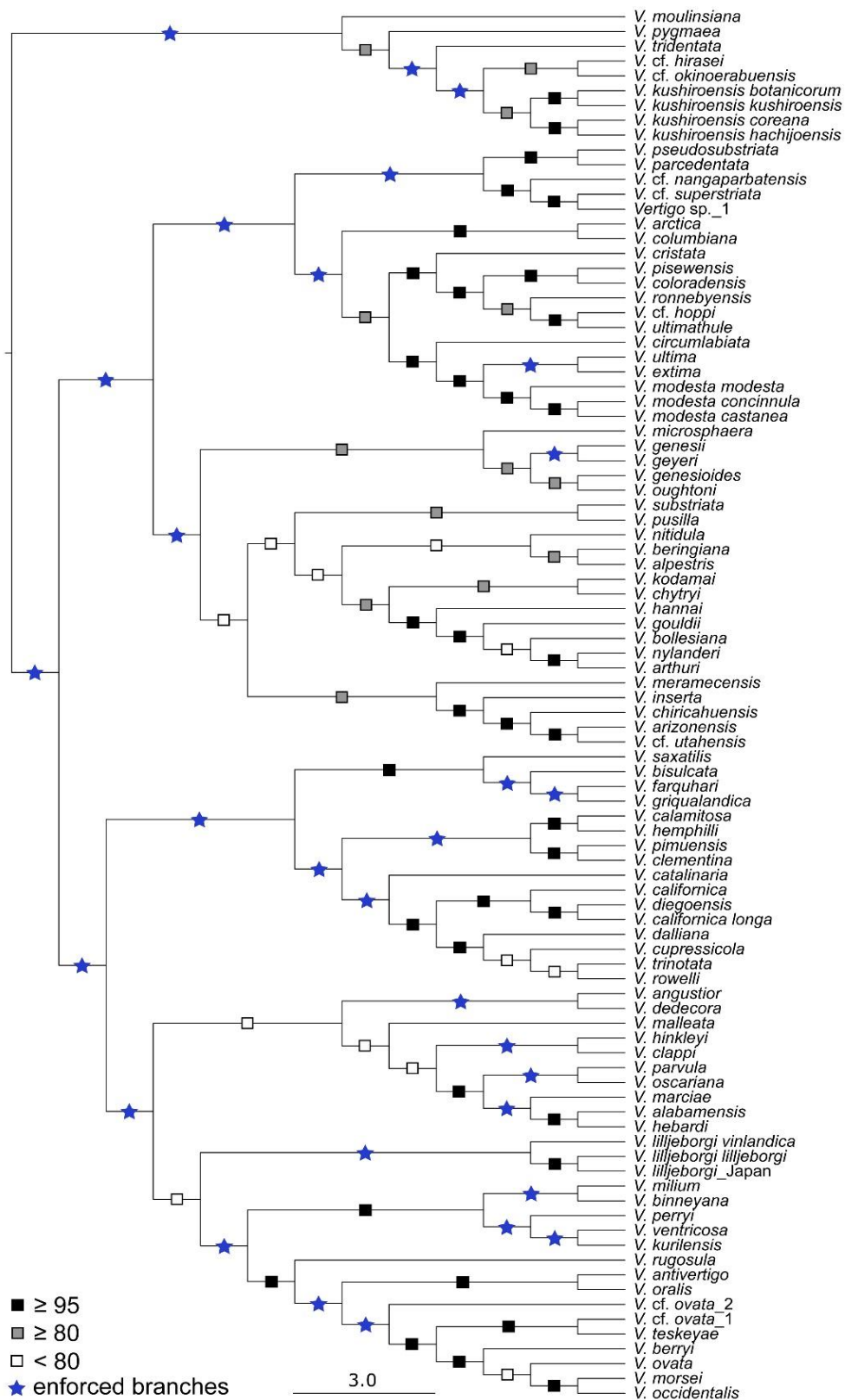


Figure S2. *Vertigo* phylogeny based on the concatenated dataset of mitochondrial (16S rRNA and COI) and nuclear (ITS1 and ITS2) markers based on Maximum Likelihood (IQTREE) analysis. Branch support was obtained through Ultrafast bootstrap; note that all enforced branches received support value of 100, except the node *V. angustior* + *V. dedecora* having the value of 99.

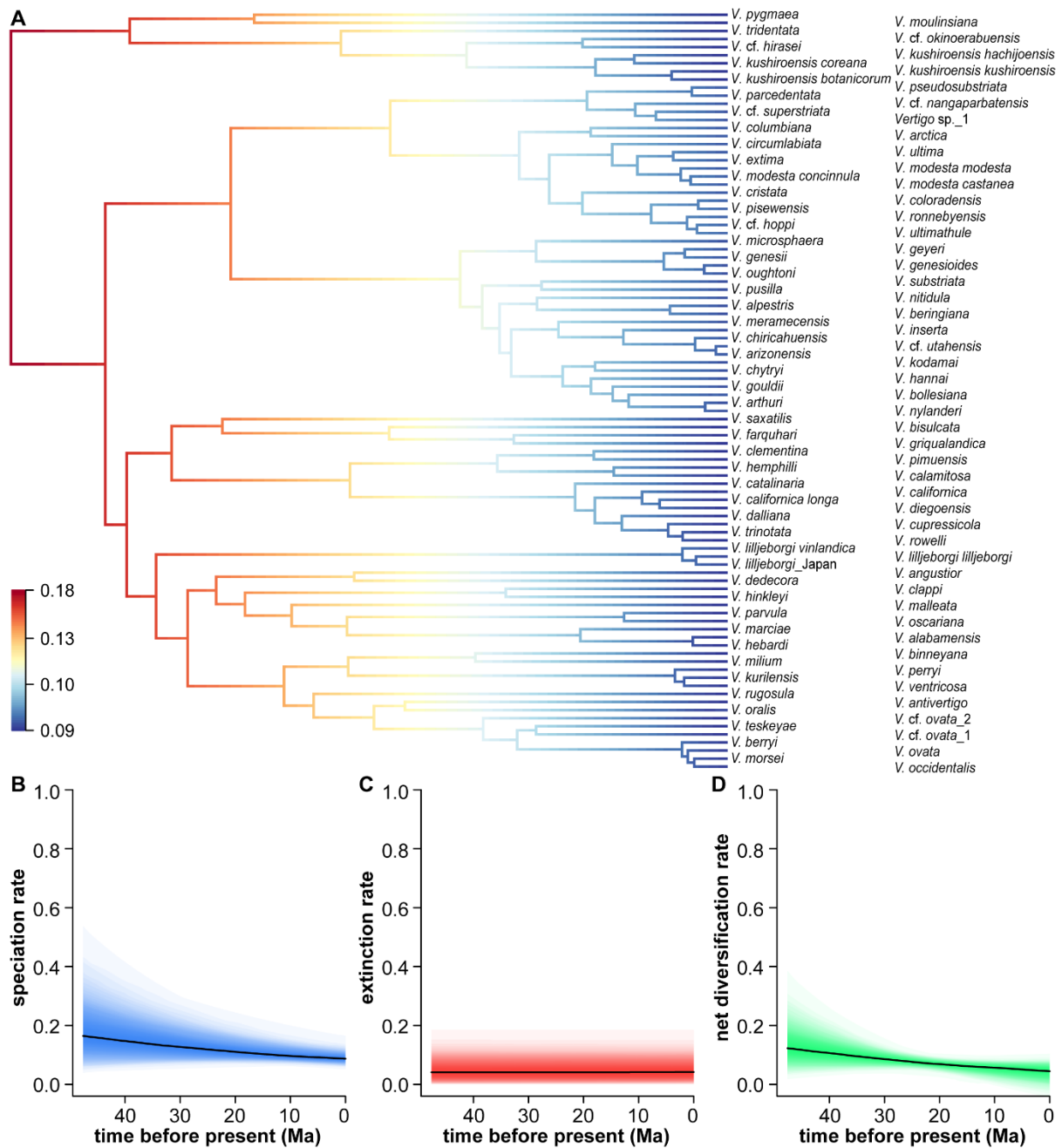
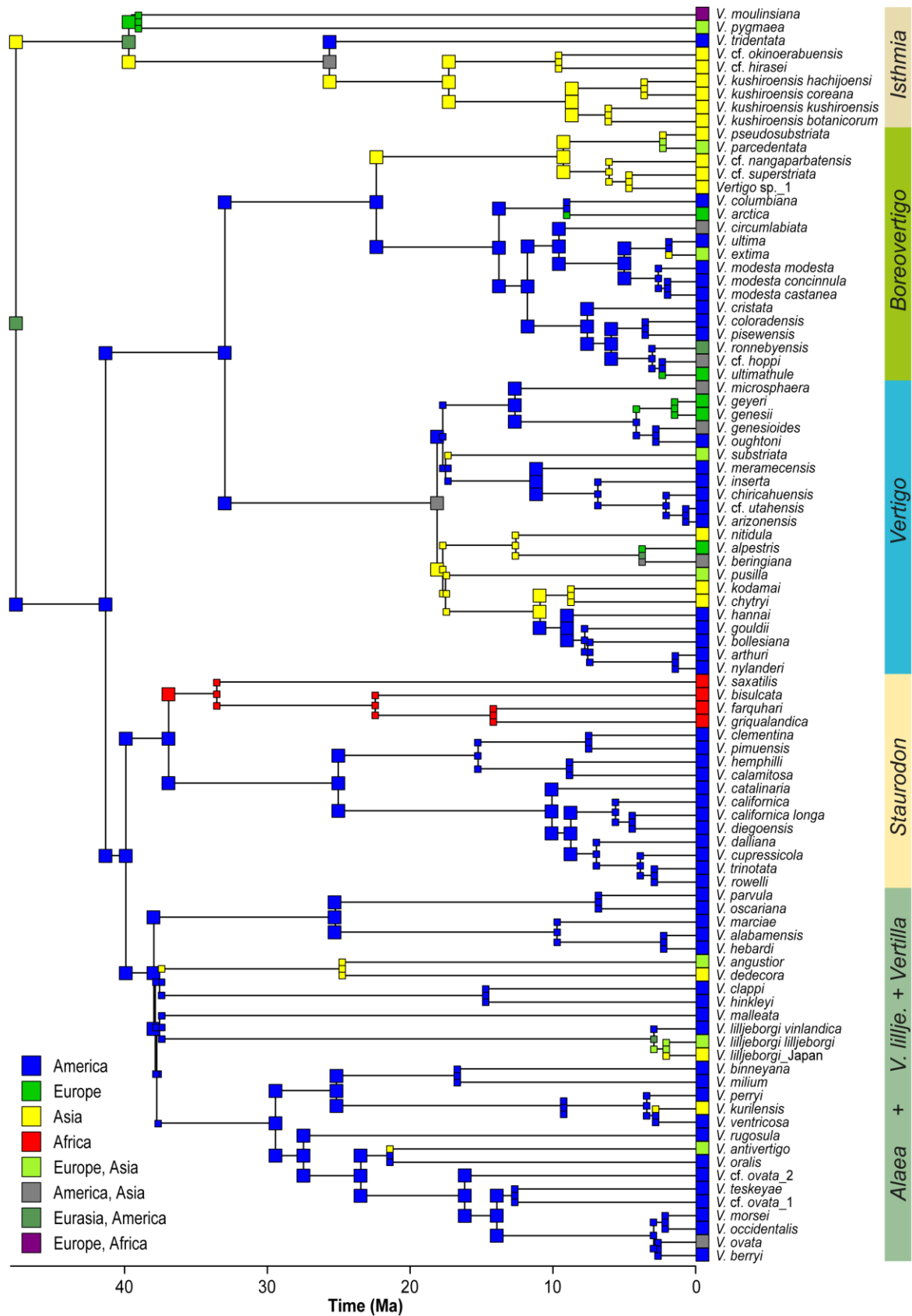


Figure S3. Diversification dynamics as reconstructed with a Bayesian analysis of macroevolutionary mixtures. **A**, Time-calibrated BEAST MCC phylogeny with branches colored according to net diversification rates, indicating the absence of major shifts in diversification rates in *Vertigo*. **B-D**, reconstructed speciation, extinction and net-diversification rates through time with in color gradient the 95% CI on each.



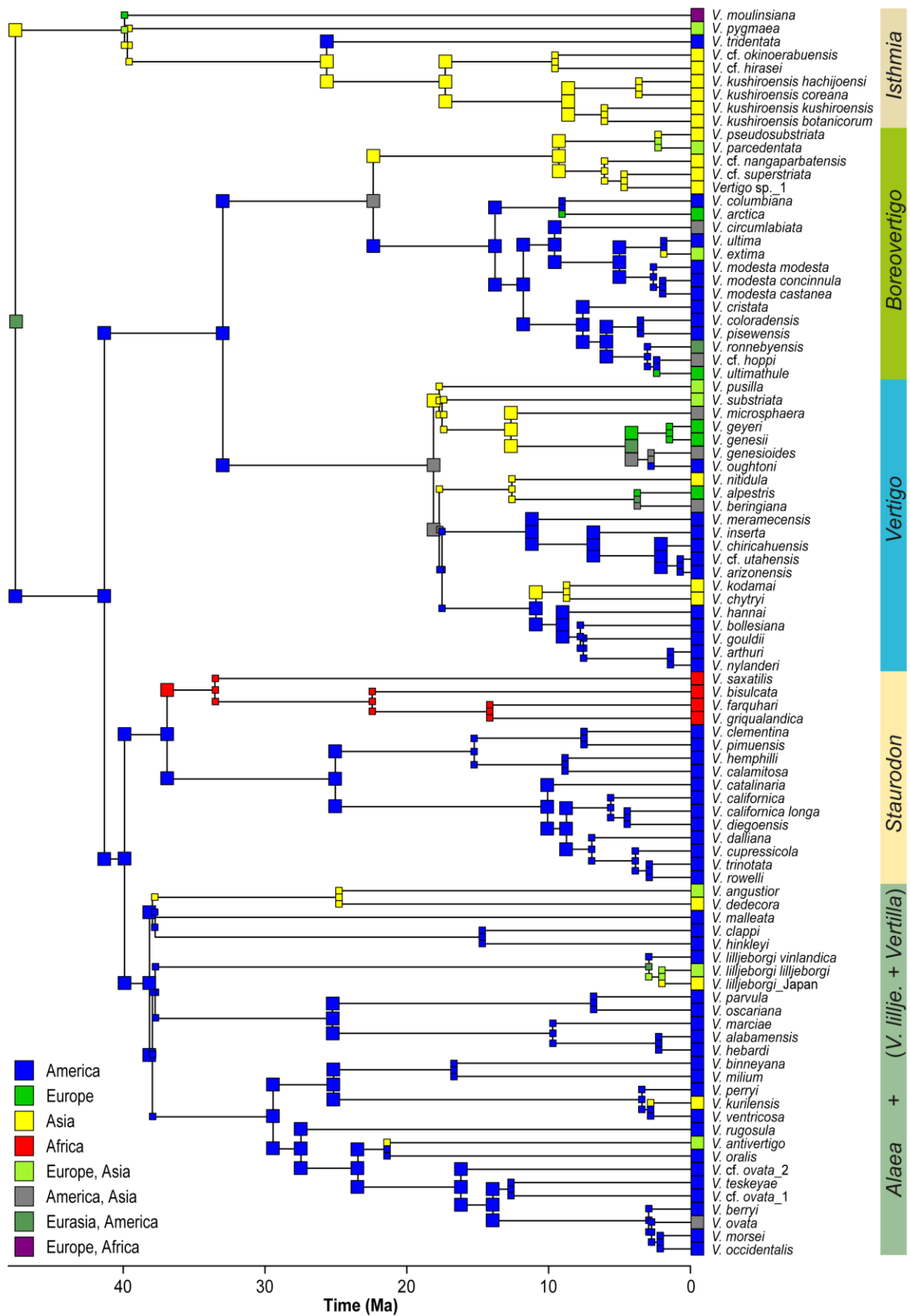


Figure S4b. Species-level phylogeny with ancestral range estimations after randomly resolving nodes that were collapsed from the BEAST MCC due to weak support (see Table S4, Tree 2). Ancestral ranges were estimated from the fit of the DEC+J model.

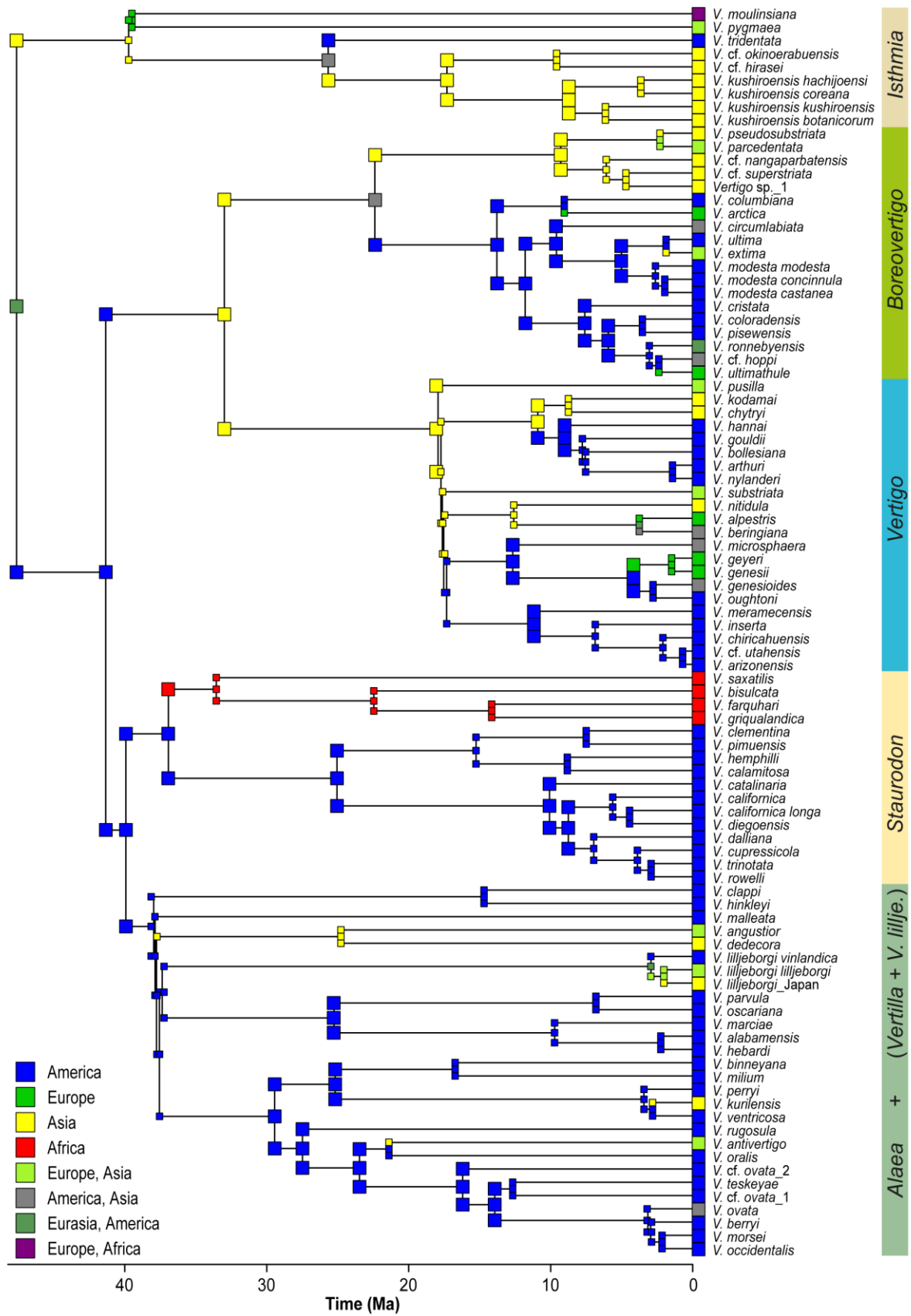


Figure S4c. Species-level phylogeny with ancestral range estimations after randomly resolving nodes that were collapsed from the BEAST MCC due to weak support see Table S4, Tree 3). Ancestral ranges were estimated from the fit of the DEC+J model.

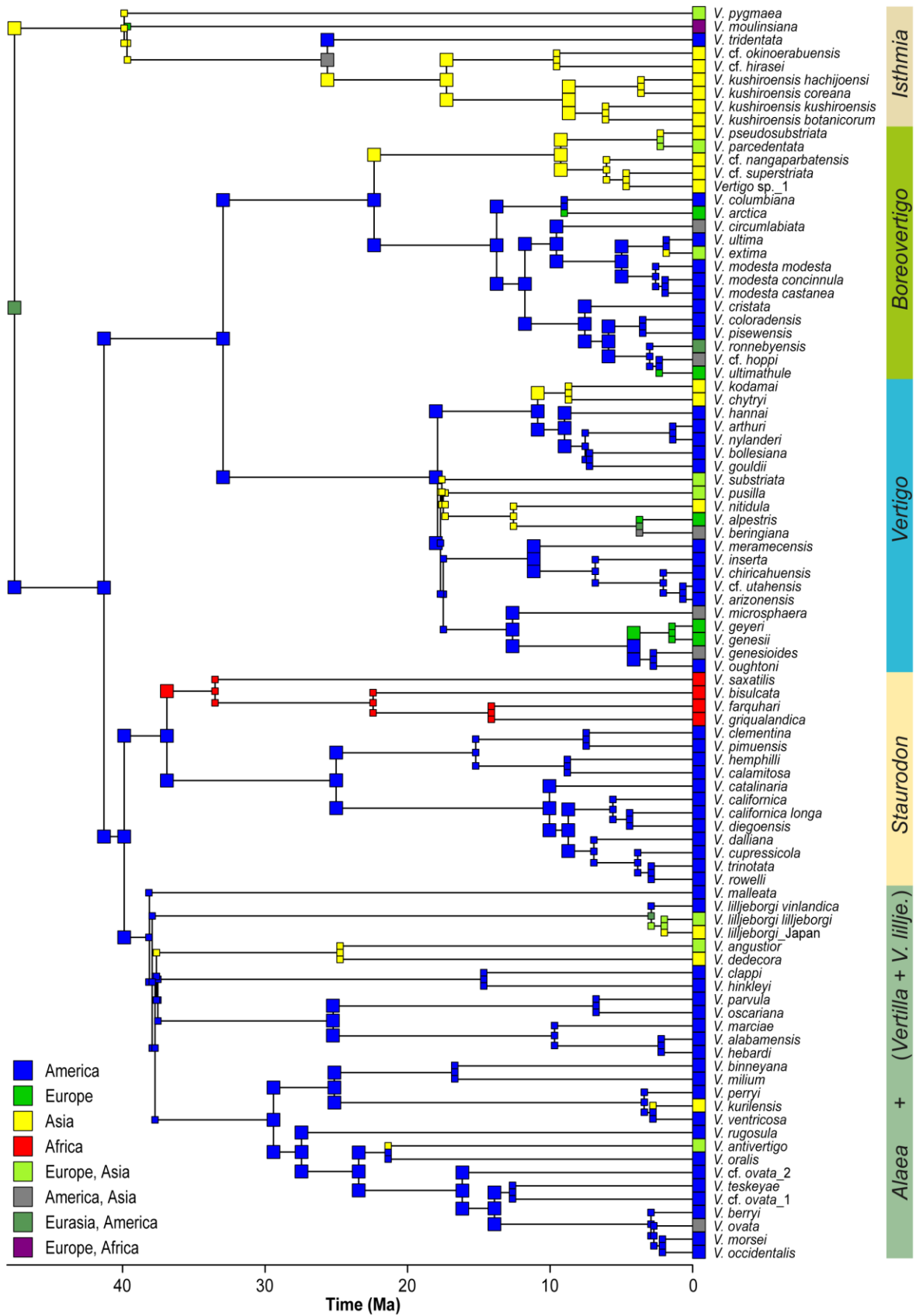


Figure S4d. Species-level phylogeny with ancestral range estimations after randomly resolving nodes that were collapsed from the BEAST MCC due to weak support (see Table S4, Tree 4). Ancestral ranges were estimated from the fit of the DEC+J model.

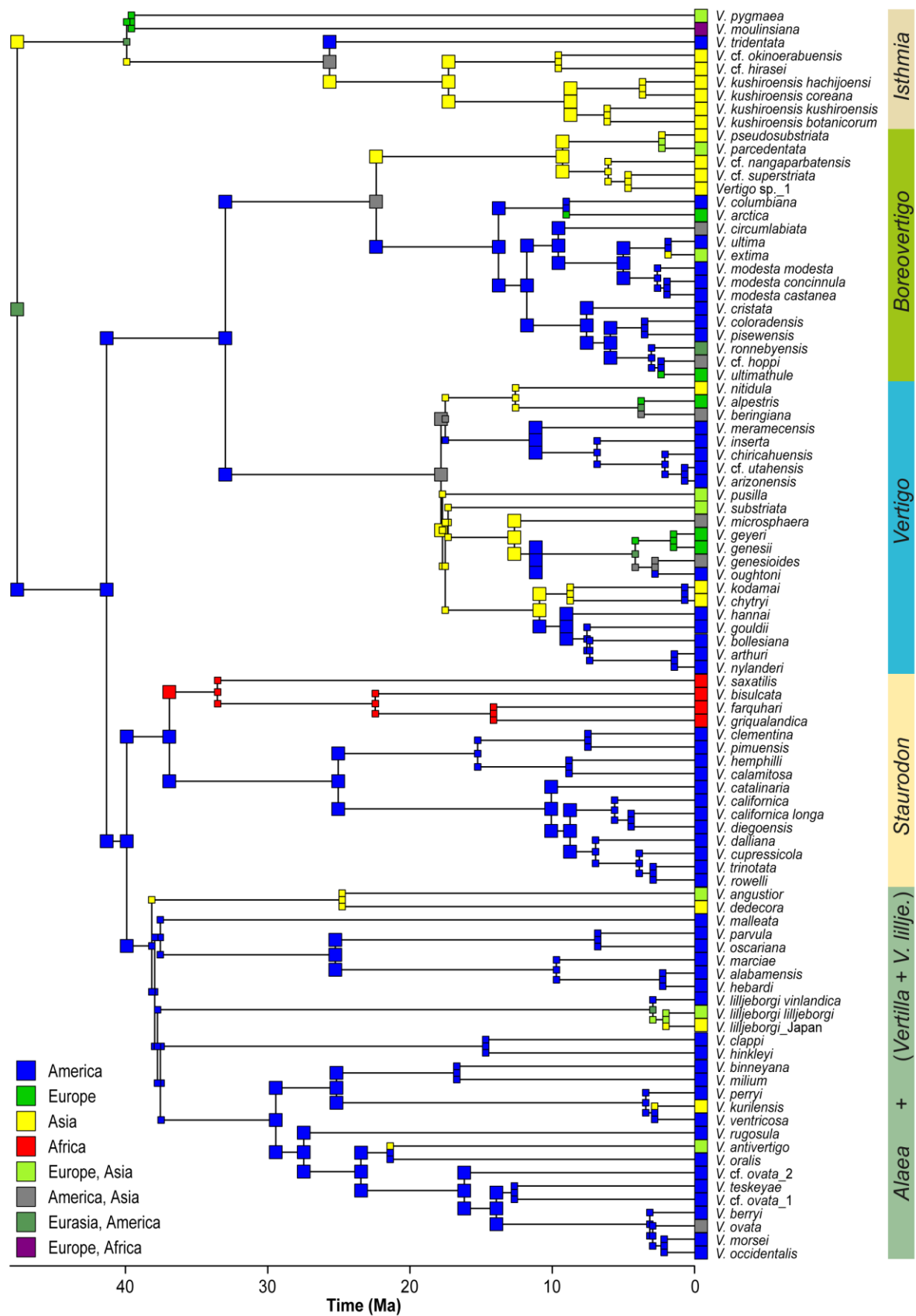


Figure S4e. Species-level phylogeny with ancestral range estimations after randomly resolving nodes that were collapsed from the BEAST MCC due to weak support (see Table S4, Tree 5). Ancestral ranges were estimated from the fit of the DEC+J model.

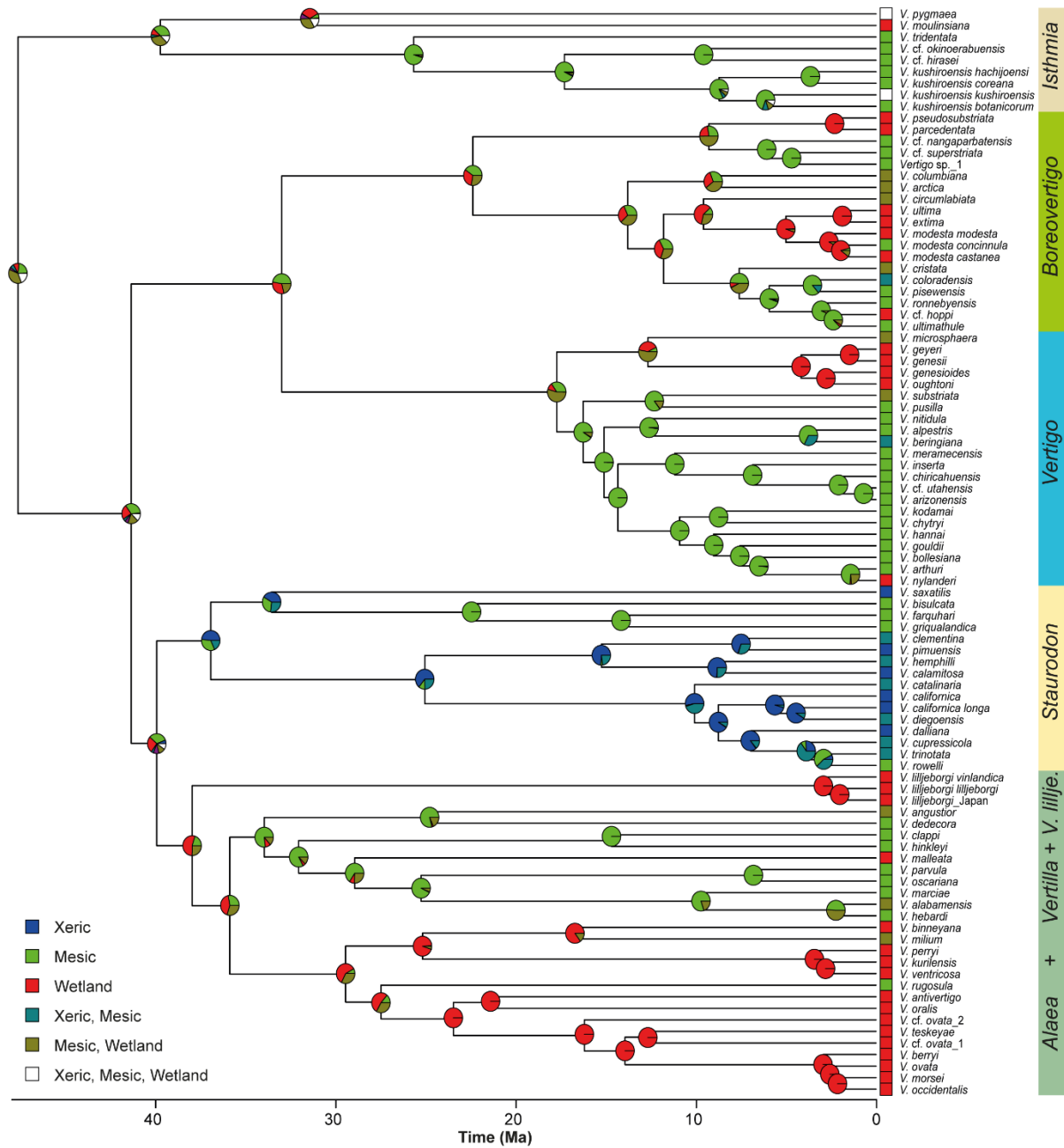


Figure S5. Reconstruction of moisture-related ecological niches along the *Vertigo* phylogeny considering a three-state discrete character allowing intraspecific polymorphism using an econiche matrix in BIOGEOBEARS.

M1. Molecular phylogenetics.

Gene fragments and alignment

Mitochondrial data consisted of fragments of 367 bp and ~450 bp of cytochrome b and 16S ribosomal RNA, respectively, and nuclear data of two fragments of the nuclear ribosomal RNA cistron, i.e. the Internal Transcribed Spacers 1 and 2, covering in total ~1300 bp. Each *Vertigo* specimen was represented across all loci; there was no missing data for the ingroup. However, the outgroup *Nesopupa* was represented by mitochondrial loci only because substantial divergence hampered reliable ITS alignment to the ingroup.

Sequences were aligned using MAFFT 7 (Kato & Standley, 2013) with the algorithm Q-INS-I, which considers the secondary structure of ncRNAs. To take advantage of the phylogenetic information contained in the gaps of the rRNA matrices, we created additional binary matrices scoring gaps as absence/presence characters in FASTGAP v1.2 (Borchsenius, 2009): one for 16S rRNA and one for ITS. This methodology has been proposed by Simmons & Ochoterena (2000), and empirical applications have shown to improve branch support and branch length estimation in Maximum Likelihood and Bayesian-based phylogenetic inference (Dessimoz & Gil, 2010; Nagy et al., 2012; Ortiz & Francke, 2016).

Mitonuclear discordance

Because the ITS and mitochondrial gene trees showed substantial topological differences for deep divergences (Figure S1), with high support in ITS and usually low or no support in the mitochondrial tree, we ran additional IQTREE analyses on the mitochondrial matrix with 30 topological constraints. Such constraints were applied for: 1) deep branches in which the ITS topology was strongly supported, and the mitochondrial tree either showed the same topology or a different topology but with low support, and 2) shallow branches showing the same topology in the ITS and mitochondrial trees, with high support in both cases (Figure S1). Then, an approximately unbiased (AU) test (Shimodaira, 2002) implemented in IQTREE showed that the constrained mitochondrial topology was statistically equivalent to the unconstrained topology ($p\text{-AU} = 0.27$), therefore rejecting mitonuclear discordance in the deepest splits of *Vertigo*. As a result, mitochondrial and nuclear data were concatenated for downstream analyses. For AU test command and results see Appendix S2.

Range estimations under topological uncertainty

For this examination, we collapsed all branches that were recovered in only one of the BEAST and IQTREE analyses or those that received low support in the abovementioned MCC tree. Subsequently, we randomly resolved the phylogeny using the *multi2di* function of APE and removed zero branch lengths by sliding nodes up to 200 ka using DISPRITY v.1.7.0 (Guillerme, 2018). The resulting branches have a length that is 32% of the minimal branch length in the MCC tree, altering regional divergence times in a way that is negligible

compared to the dating uncertainty. We performed biogeographic analyses with a pool of randomly resolved phylogenies.

References

- Borchsenius, F. (2009). FastGap 1.2. Available at: https://www.aubot.dk/FastGap_home.htm.
- Dessimoz, C., Gil, M. (2010). Phylogenetic assessment of alignments reveals neglected tree signal in gaps. *Genome Biology*, *11*, 1–9.
- Guillerme, T. (2018). dispRity: A modular R package for measuring disparity. *Methods in Ecology and Evolution*, *9*, 1755–1763.
- Katoh, K., Standley, D. M. (2013). MAFFT multiple sequence alignment software version 7: Improvements in performance and usability. *Molecular Biology and Evolution*, *30*, 772–780.
- Nagy, L. G., Kocsubé, S., Csanádi, Z., Kovács, G. M., Petkovits, T., Vágvölgyi, C., Papp, T. (2012). Re-mind the gap! Insertion - deletion data reveal neglected phylogenetic potential of the nuclear ribosomal internal transcribed spacer (ITS) of fungi. *PLoS ONE*, *7*, e49794.
- Ortiz, D., Francke, O. F. (2016). Two DNA barcodes and morphology for multi-method species delimitation in *Bonnetina tarantulas* (Araneae: Theraphosidae). *Molecular Phylogenetics and Evolution*, *101*, 176–193.
- Shimodaira, H. (2002). An approximately unbiased test of phylogenetic tree selection. *Systematic Biology*, *51*, 492–508.
- Simmons, M. P., Ochoterena, H. (2000). Gaps as characters in sequence-based phylogenetic analyses. *Systematic biology*, *49*, 369–381.

M2. Seven ingroup fossil calibration points (see also Table S3).

1. Oldest *Vertigo*. The fossil record of *Vertigo* goes back to earliest Middle Eocene, ca 50 Ma ago (Good, 1987; Harzhauser & Neubauer, 2021). The earliest record of an unambiguous *Vertigo* species is *Vertigo* cf. *arenula* reported by Good (1987) from the Bridgerian (50.3-46.2 Ma; earliest Middle Eocene) in east central Nevada (USA). This fossil clearly resembles modern members of the genus as to the shape and size of its shell along with the presence of mouth lamellae (Fig. 2R; Good, 1987). This fossil was dated based on mollusc biostratigraphy and the co-occurrence with Bridgerian mammalian species. Associated age divisions are adapted from Barnosky et al. (2014). Additional fossils that unambiguously belong to *Vertigo* were recovered from Baltic amber of the Lutetian (~44 Ma), namely *Vertigo hauchecornei* and *V. kuenowii* (Harzhauser & Neubauer, 2021). Note that *Vertigo (Isthmia) palangula* (de Boissy, 1848) as described from the Thanetian (59.2-56.0 Ma) from France is slightly older, however, taxonomically relevant features of the shell such as loose coiling, the apertural shape, and the lip development clearly distinguish it from all known *Vertigo* species. In shell architecture, *V. palangula* resembles representatives of the genus *Pupoides* Pfeiffer, 1854, which is genetically distinct from *Vertigo* (Saadi et al., 2021). Nevertheless, as we used a uniform prior from 87 to 50 Ma for the most recent common ancestor (MRCA) of *Vertigo* our prior included scenarios consistent with a Thanetian or somewhat older origin of the genus.

2. Oldest *Vertigo* of the subgenus *Vertilla*. The fossil *Vertigo vectensis* Cox, 1924 was described from the Bembridge limestone of Priabonian age (37.7-33.9 Ma; late Eocene) from the Isle of Wright, UK (Cox, 1924). Recently, other specimens of this fossil species have been reported from two other outcrops of the same strata (Harzhauser & Neubauer, 2021). The small size (shell height 1.7 mm), ovate shape (width 1.2 mm), and notably small aperture allow to assign this fossil to the subgenus *Vertilla* (Nekola et al., 2018). As the topology in our phylogeny is poorly supported near the stem of *Vertilla*, we used *V. vectensis* to calibrate the directly stemwards well-supported node, i.e. the MRCA of *V. lilljeborgi*, *Vertilla* and *Alaea*.

3. Oldest *Vertigo* of the subgenus *Alaea*. There is abundant fossil material from the upper Oligocene strata across Europe and North America that resembles extant members of the subgenus *Alaea* (sensu Nekola et al., 2018). The oldest related records have been reported from the Hochheim-Flörsheim beds in Germany (lot no. 152162, Senckenberg Museum) and have been assigned to *Vertigo ovatula* (Sandberger, 1875). These beds would have been deposited in the Chattian, between 27.8 and 23.0 Ma (Stworzewicz, 1999; Harzhauser & Neubauer, 2021). Based on its shell features *V. ovatula* was considered to be closely related to the extant American *V. ovata* or *V. milium* (Stworzewicz, 1999). Our phylogeny recovers both of these extant species within the subgenus *Alaea*, but in distant phylogenetic positions from one another. The ovate shell of *V. ovatula* is of small size and has 7-6 lamellae in its widely open aperture, which allow unambiguous attribution to the subgenus *Alaea*. As such, *V. ovatula* has been used to date the stem of the subgenus *Alaea*.

4. Split of *Vertigo angustior* from *V. dedecora*. The extant species *V. angustior* bears unique shell features that easily distinguish it from all other extant members of the genus. Most of

the diagnostic features for *V. angustior* are also found in *V. oecsis* (Halaváts, 1911), a fossil species described from the Upper Pannonian in Hungary. Because of this resemblance, *V. oecsis* has long been considered to be a subspecies of *V. angustior* Jeffreys, 1830. Fossils attributed to *V. oecsis* or *V. angustior* have been commonly found in Tortonian sediments across Central Europe, with the oldest known specimen dated to 15.97-12.70 Ma (Harzhauser & Neubauer, 2021).

5. Split of *Vertigo parcedentata* and *V. pseudosubstriata*. Numerous Pleistocene records of *V. parcedentata* have been found in Eurasian from loess deposits of various glacial cycles. Morphologically, these fossils are indistinguishable from extant *V. parcedentata* (Ložek, 1964, Moine, 2014). The oldest occurrence is from the oldest glacial unit of the southern Polish complex (Narevian=Menapian, 1.2 Ma) (Stworzewicz et al., 2012). As such, this fossil was used to date the split of *V. parcedentata* from its sister species *V. pseudosubstriata*.

6. Split of *Vertigo genesii* and *V. geyeri*. Numerous records of *V. genesii* have been found across Europe in Pleistocene loess deposits from various glacial cycles. The oldest record of *V. genesii* are from the oldest glacial unit of the southern Polish complex, together with the abovementioned *V. parcedentata* (Narevian=Menapian, 1.2 Ma) (Stworzewicz et al., 2012). These fossils are indistinguishable from extant *V. genesii*, and as such they were used to date the split between *V. genesii* and *V. geyeri*.

7. Split of *Vertigo nylanderii* and *V. arthuri*. The oldest fossil identified as *V. nylanderii* was reported from west-central Illinois in sediments for which the minimum age is constrained by the age of the Brunhes/Matuyama magnetic reversal (Miller et al., 1994).

References

- Barnosky, A. D., Holmes, M., Kirchholtes, R., Lindsey, E., Maguire, K. C., Poust, A. W., Stegner, M. A., Sunseri, J., Swartz, B., Swift, J., Villavicencio, N. A., and Wogan, G. O. U. (2014). Prelude to the Anthropocene: Two new North American Land Mammal Ages (NALMAs): *The Anthropocene Review*, v. 1, p. 225–242, doi: 10.1177/2053019614547433.
- Cox, L. R. (1924). *Vertigo vectensis*, n. sp., from the Bembridge Limestone, Isle of Wight. *Journal of Molluscan Studies*, 16, 123-124.
- Ložek, V. (1964). *Quartärmollusken der Tschechoslowakei*. Nakladatelství Československé akademie věd.
- Miller, B. B., Graham, R. W., Morgan, A. V., Miller, N. G., McCoy, W. D., Palmer, D. F., Smith, A. J., Pilny, J. J. (1994). A biota associated with Matuyama-age sediments in west-central Illinois. *Quaternary Research*, 41, 350–365.
- Moine, O. (2014). Weichselian Upper Pleniglacial environmental variability in north-western Europe reconstructed from terrestrial mollusc faunas and its relationship with the presence/absence of human settlements. *Quaternary International*, 337, 90–113.
- Stworzewicz, E. (1999). Miocene land snails from Belchatow (Central Poland). IV. Pupilloidea (Gastropoda Pulmonata). Systematic, biostratigraphic and palaeoecological studies. *Folia Malacologica*, 7, 133–170.

- Stworzewicz, E., Granoszewski, W., Wójcik, A. (2012). Malacological and palynological evidence of the Lower Pleistocene cold phase at the Carpathian Foothills (Southern Poland). *Quaternary Research*, 77, 492–499.
- Saadi, A. J., Mordan, P. B., Wade, C. M. (2021). Molecular phylogeny of the Orthurethra (Panpulmonata: Stylommatophora). *Zoological Journal of the Linnean Society*, 193, 1126–1140.